analytical chemistry

Article

pubs.acs.org/ac

Quantum Dot Nanometal Surface Energy Transfer Based Biosensing of Sialic Acid Compositions and Linkages in Biological Samples

Raghavendra Kikkeri,[†,∥] Vered Padler-Karavani,[†,⊥] Sandra Diaz,[†] Andrea Verhagen,[†] Hai Yu,[‡] Hongzhi Cao,[‡,▽] Martijn A. Langereis,[§,○] Raoul J. De Groot,[§] Xi Chen,[‡] and Ajit Varki*[,†]

[†]Glycobiology Research and Training Center, Departments of Medicine and Cellular and Molecular Medicine, University of California, San Diego, La Jolla, California, United States

[‡]Department of Chemistry, University of California, Davis, California 95616, United States

[§]Virology Division, Department of Infectious Diseases and Immunology, Faculty of Veterinary Medicine, Utrecht University, Yalelaan 1, 3584 CL Utrecht, The Netherlands

Supporting Information

ABSTRACT: Current methods for analyzing sialic acid diversity in modifications and linkages require multistep processing, derivatization, and chromatographic analyses. We here report a single-step optical method for identification and quantification of different compositions of sialoglycans on glycoproteins and in serum. This was achieved by measuring and quantifying nanometal surface energy transfer (NSET) signals between quantum dots and gold nanoparticles bound to specific sialic acid binding proteins (SBPs) and sialic acid moieties, respectively. The biosensing process is based on the NSET turn-on by external sialic acid species that compete for binding to the SBPs. Selectivity of the biosensor toward sialoglycans can be designed to detect the total amount, glycosylation linkages (α2−6 vs α2−3), and modifications (9-*O*-acetyl and *N*-glycolyl groups) in the samples. This nanobiosensor is a prototype expected to achieve limits of the detection down to the micromolar range for high-throughput quantification and analysis of different compositions of sialoglycans present in biological or biomedical samples.

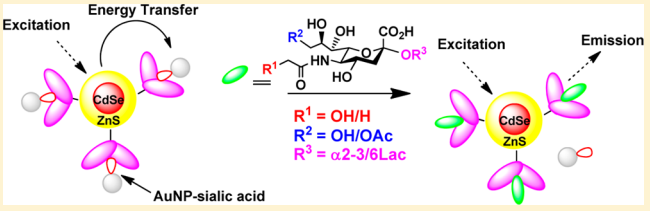

Sialic acids (Sias) are a class of monosaccharides typically found at the terminal location of *N*-glycans, *O*-glycans, and glycosphingolipids (and occasionally capping side chains of GPI anchors) in animals of the *Deuterostome* lineage, and in certain bacteria that associate with them.[1] One of the most striking features of Sias is their structural diversity, with about 50 Sia species known, consisting of *N*-acetylneuraminic acid (Neu5Ac), *N*-glycolylneuraminic acid (Neu5Gc), keto-deoxy-nonulosonic acid (Kdn), and their derivatives modified by acetylation, lactylation, methylation, and/or sulfation.[2] In vertebrates, Sias mediate a wide variety of biological roles, many of which are affected by the modifications and/or linkages of Sias.[3] For example, the role of CD22 in modulating B cell receptor (BCR) signaling depends on recognition of α2−6-linked Sias,[4] and invasion by certain viruses also depends on Sia linkages and/or the presence of Sia-O-acetylation.[5] Altered sialylation is also a feature of a number of cancers.[6] Recently we have shown that the nonhuman Sia Neu5Gc is metabolically assimilated from dietary sources onto human cell surfaces and causes antigen−antibody mediated chronic inflammation, which can potentially facilitate disease processes such as tumor progression[7] and vascular inflammation,[8] as well as provide epitopes for antibodies as novel cancer biomarkers and immunotherapeutics.[9] Findings such as these have increased efforts to develop efficient methodologies to quantify sialic acid compositions in biological samples. Most chemosensor methods exploit the interaction between boronic acid and the hydroxyl groups of sialic acids. The drawback of such systems is the nonspecific binding to vicinal cis-diol derivatives.[10] In contrast, 1,2-diamino-4,5-methylenedioxybenzene (DMB) derivatization followed by reversed-phase high-performance liquid chromatography (RP-HPLC) is most useful for determining labile sialic acids. However, chemical derivatization is necessary to meet detection requirements, and there are multiple steps involved.[11]

Recently, nanotechnology-based biosensors with improved speed, low cost, and direct readout results have been developed as new approaches for the detection of carbohydrates.[12] We present here the utility of the quantum dot nanometal surface energy transfer (QD-NSET) technique to detect and quantify different compositions of sialoglycans containing diverse sialic acid forms in biological samples. NSET is an efficient quenching technique occurring at distances nearly twice as far as fluorescence resonance energy transfer (FRET).[13a] This technique has been extensively used to measure distance for protein interaction on DNA and a Hg(II) sensor.[13] In our method, NSET between QDs and gold nanoparticles (AuNPs)

Received: October 9, 2012
Accepted: March 15, 2013
Published: March 15, 2013

   dx.doi.org/10.1021/ac400320n | *Anal. Chem.* 2013, 85, 3864−3870

is propagated by specific sialic acid-binding protein−carbohydrate interactions and biosensing is based on the switching-on of QD fluorescence by adding sialic acids or sialic acid-containing glycoconjugates that compete for binding to the Sia-binding protein (SBP) and therefore remove the quencher AuNP (Figure 1i). To profile sialic acid compositions in

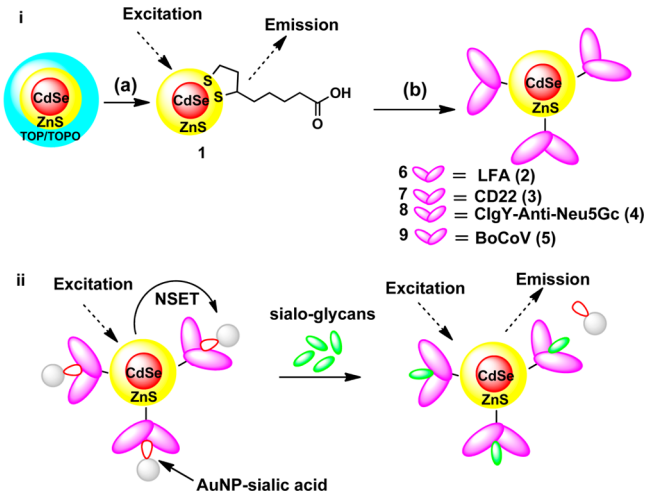

Figure 1. (i) Synthesis of sialic acid binding protein conjugated quantum dots **6**−**9**: (a) DL-thioctic acid/$NaBH_4$/EtOH; (b) EDC/NHS/H_2O/sialic acid binding proteins (LFA, CD22, CIgY-Anti-Neu5Gc, BoCoV). (ii) Schematic illustration of the NSET-based sialic acid biosensor principles: QDs (**6**−**9**) were treated with different AuNPs (**13**−**15**) carrying sialic acid residues (**10**−**12**) to generate NSET-based photoluminescence quenching of QDs **6**−**9**. Finally, the NSET was disturbed by adding external sialoglycans having strong affinity to SBP (**2**−**5**).

biological samples, four SBPs with distinct binding specificity to sialic acid species were immobilized on QDs and reacted with PEGylated gold nanoparticles carrying Neu5Ac/Neu5Gc sugar moieties with or without 9-*O*-acetyl modifications.[9,14] Limax flavus agglutinin (LFA), CD22 (Siglec-2), chicken-IgY anti-Neu5Gc (CIgY-Anti-Neu5Gc), and bovine coronavirus HE^0 (BoCoV) were selected as SBPs (Figure 1; SBP 2, 3, 4, and 5, respectively, yielding QD6, QD7, QD8, and QD9). While LFA is a lectin that binds to all common sialic acids,[15] human CD22-Fc is specific to Neu5Ac/Neu5Gcα2−6-linked sialic acids,[16] BoCoV is specific to 9-O-acetylated sialic acids,[17] and chicken anti-Neu5Gc-IgY is specific to the nonhuman sialic acid Neu5Gc.[18]

Our results indicate that the QDs-based biosensor requires only a small amount of biomaterials (micromolar range) and provides high selectivity and sensitivity for different composition of sialoglycans, rendering this method attractive.

RESULTS AND DISCUSSION

Synthesis of Sialic Acid Functionalized Nanoparticles. Cadmium selenide/zinc sulfide (CdSe/ZnS) cores with SBPs were prepared starting from ligand exchange with thioctic acid and tri-*n*-octyl phosphine/tri-*n*-octyl phosphine oxide (TOP/TOPO)-capped QDs to afford QD−COOH (**1**).[19] The terminal carboxylic acid of **1** was further reacted with 1-ethyl-3-(3-dimethylaminopropyl) carbodiimide and *N*-hydroxysuccinimide (NHS), before conjugating with LFA, CD22, CIgY-Anti-Neu5Gc, and BoCoV (**2**−**5**) to yield QDs **6**−**9**, respectively (Figure 1). The conjugated QDs were purified by filtering with a Microcon centrifugal filter device with a cutoff range of 30 kDa. The concentration of protein on CdSe/ZnS was determined by the BCA assay using a microtiter plate. QDs **6**−**9** showed 6−7 protein molecules per quantum dot. The gold nanoparticles were obtained by adding a methanol solution of SH−PEG_{2000}−COOH to an aqueous solution of tetrachloroauric acid ($HAuCl_4$) (Figure 2). By reduction of the resulting

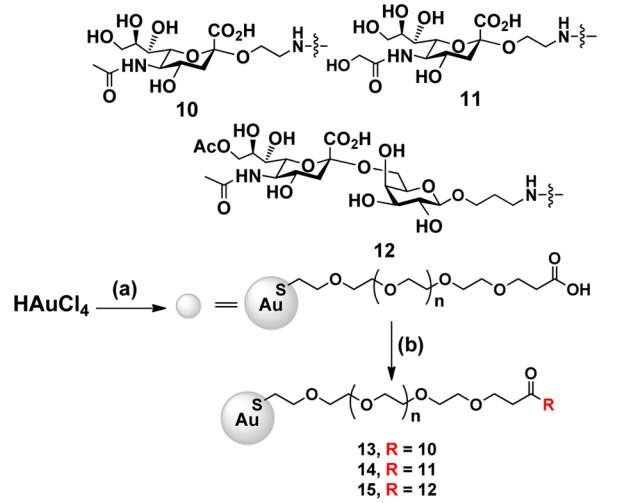

Figure 2. Synthesis of gold nanoparticles **13**−**15**: (a) sodium borohydride/SH−PEG−COOH; (b) Comp **10**−**12**/WSC/NHS.

mixture with $NaBH_4$, a yellow to dark brown suspension was immediately formed. The suspension was shaken for about 2 h, and the solvent was then removed. The nanoparticles were purified by centrifugal filtering and characterized by ^1H and ^{13}C NMR and UV−vis spectroscopy.[19d] The terminal carboxylic acid was further reacted with sialic acid species **10**−**12** (Figure 2) to yield nanoparticles AuNPs **13**−**15**, respectively. The concentration of sialic acids on AuNPs was determined by acid hydrolysis followed by the DMB-HPLC method, indicating that there were 15−18 sialic acid moieties per AuNP.

After synthesizing QDs and AuNPs, the fluorescence quenching efficiency can be quantified by the Stern−Volmer equation.

$$F_0/F = 1 + K_{SV}[\text{AuNP}] \quad (1)$$

F_0 and F denote the steady-state fluorescence intensities in the absence and presence of the quencher AuNPs, respectively. A plot of F_0/F versus [AuNPs] produced a straight line, as shown in Figure 3, the slope of which gave the Stern−Volmer quenching constant. The experimental values of K_{SV} of QDs **6**−**9** with respect to AuNPs **13**−**15** are given in the Supporting Information, Tables S1 and S2.

Although the quenching efficiency is quite high, the lack of localized surface plasma resonance (LSPR) of AuNPs **13**−**15** in the UV−vis absorption spectra suggests the absence of a FRET mechanism (Supporting Information, Figure S3). Instead of FRET, nanometal surface energy transfer (NSET) has been highly successful in describing the fluorescence quenching by small gold nanoparticles.[13] Recent studies show that NSET does not require a resonance interaction between the donor−acceptor probes. According to the Persson and Lang theory, AuNPs[17a] with a limited size and surface will accept only a limited amount of energy by the formation of electron−hole pairs near the surface.

dx.doi.org/10.1021/ac400320n | *Anal. Chem.* 2013, 85, 3864−3870

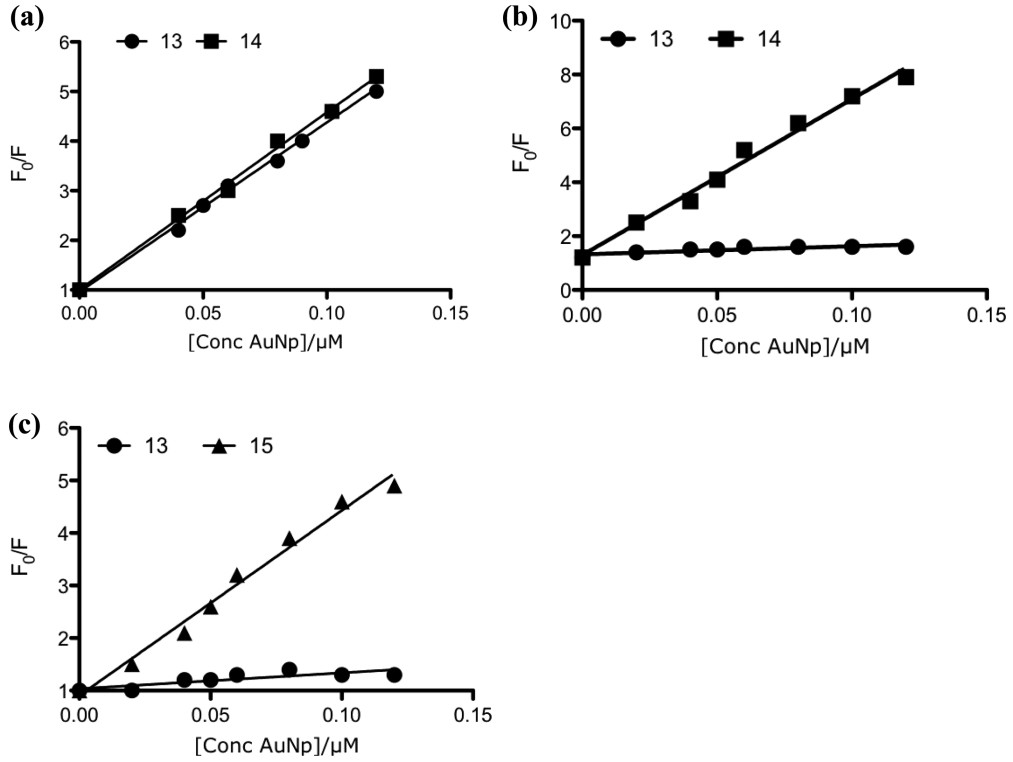

Figure 3. Stern–Volmer plot of F_0/F vs [AuNPs]: (A) [QD-**6**] = 6 nM, [Au-**13**/**14**] = 0–150 nM in PBS solution, pH = 7.4, incubation time = 1 min; (B) [QD-**8**] = 6 nM, [Au-**13**/**14**] = 0–200 nM in PBS solution, pH = 7.4, incubation time = 1 min; (C) [QD-**9**] = 6 nM, [Au-**13**/**15**] = 0–150 nM in PBS solution, pH = 7.4, incubation time = 1 min.

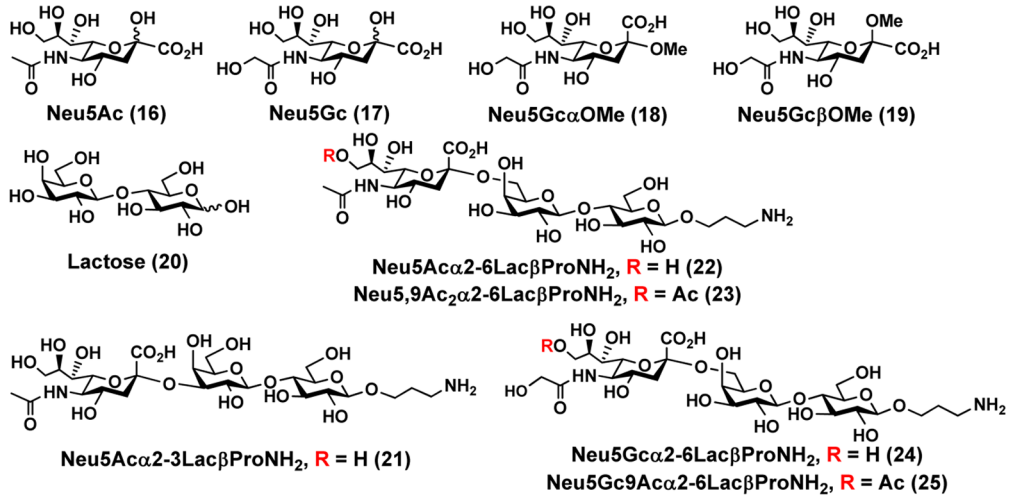

Figure 4. Chemical structures of sialic acid residues used for biosensing process (**16**–**25**).

To validate the mechanism of energy transfer from the QDs to the gold nanoparticles, we have examined the separation distance (d_0) at which the energy transfer efficiency is 50%. For the NSET mechanism, d_0 can be quantified by eq 2.

$$d_{0(\mathrm{NSET})} = \left\{ \frac{0.225\Phi_{\mathrm{QD}}}{\omega_{\mathrm{QD}}{}^2 \omega_{\mathrm{F}} k_{\mathrm{F}}} c^3 \right\}^{1/4} \quad (2)$$

Φ_{QD} denotes the quantum yield of the QDs **6**–**9** in the absence of acceptor, $\omega_{\mathrm{QD}}{}^2$ and c are the angular frequency of the donor emission and velocity of light, and $\omega_{\mathrm{F}} = 1.2 \times 10^8$ cm^{-1} and $k_{\mathrm{F}} = 8.4 \times 10^{15}$ rad/s are the bulk gold angular frequency and Fermi vector, respectively. The d_0 value in the NSET was calculated to be 6.33 ± 0.3 nm from eq 2 for QD-**6** and AuNP-**13**, and this value is better fit to the NSET model of quenching compared to FRET.[13] This is due to the lack of a pronounced LSPR dipole absorption necessary for FRET.

Furthermore, the quenching constant derived for QDs **6** and **7** was almost the same as the quenching constant with AuNPs **13** and **14** quenchers. QDs **8** and **9** showed preferential quenching with particles **14** and **15**, respectively, likely related to preferential binding with the nonhuman sialic acid Neu5Gc and 9-OAc-sialic acid, respectively (Supporting Information, Table S2). On the basis of these results, we constituted four donor/acceptor (NSET-1 (**6**/**13**); NSET-2 (**7**/**13**); NSET-3 (**8**/**14**), and NSET-4 (**9**/**15**) models at an optimal concen-

dx.doi.org/10.1021/ac400320n | Anal. Chem. 2013, 85, 3864–3870

Table 1. Analytical Parameters (Low Detection Limit, DL; Detection Range, DR) Related to Determination of Different Sialic Acid Species with NSET Mixtures[a]

sialic acid samples	NSET-1 DL and (DR) in nM	NSET-2 DL and (DR) in nM	NSET-3 DL and (DR) in nM	NSET-4 DL and (DR) in nM
16	105 ± 4 (100−600)	N.M.	N.M.	N.M.
17	156 ± 5 (150−780)	N.M.	N.M.	N.M.
18	28 ± 1 (30−400)	N.M.	N.M.	N.M.
19	310	N.M.	N.M.	N.M.
20	N.M.	N.M.	N.M.	N.M.
21	0.5 ± 0.3 (1−285)		N.M.	N.M.
22	0.5 ± 0.2 (1−285)	0.2 ± 0.1 (1−175)		
23	N.M.	N.M.	N.M.	1.2 ± 0.5 (2−175)
24	0.5 ± 0.2 (1−290)	0.3 ± 0.2 (1−175)	0.2 ± 0.2 (1−140)	
25	N.M.	N.M.	0.4 ± 0.2 (1−140)	1.2 ± 0.5 (2−175)

[a]Error bar represents standard deviation from the means of three experiments. N.M. is not measured.

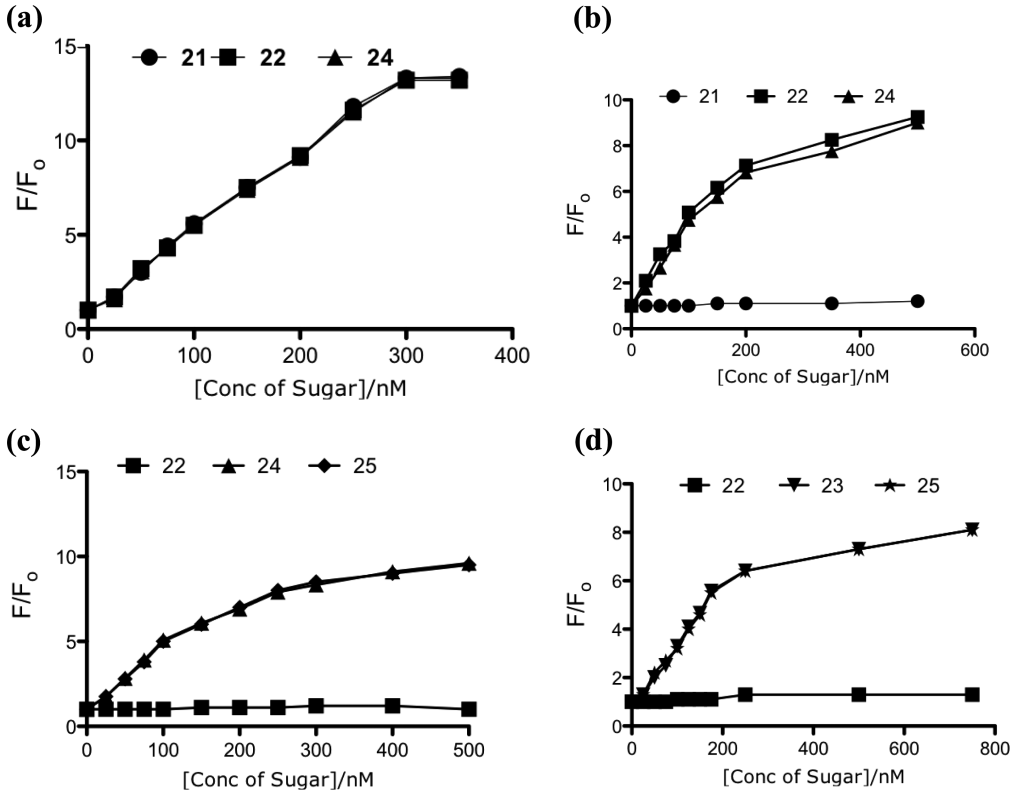

Figure 5. Sialic acid biosensor using different donor/acceptor compositions. (a) Fluorescence increase of NSET-1 (QD-**6**/Au-**13**) in presence of increasing concentrations of sialic acid residues (**21**−**25**) [QD-**6**] = 6 nM, [Au-**13**] = 110; total volume 100 μL, PBS pH = 7.4; incubation time = 1 h; RT; [**21**/**22**/**24**] = 0−350 nM; incubation time = 1 min; λ_{exc} = 450 nm; λ_{em} = 640 nm. (b) NSET-2 (QD-7/Au-**13**): [QD-7] = 6 nM [Au-**13**] = 130 nM; total volume 100 μL, PBS pH = 7.4; incubation time = 1 h; RT; [**21**/**22**/**24**] = 0−500 nM; incubation time = 1 min; λ_{exc} = 450 nm; λ_{em} = 640 nm. (c) NSET-3 (QD-**8**/Au-**14**): [QD-**8**] = 6 nM, [Au-**14**] = 120 nM; total volume 100 μL, PBS pH = 7.4; incubation time = 1 h; RT; [**22**/**24**/**25**] = 0−300 nM; incubation time = 1 min; λ_{exc} = 450 nm; λ_{em} = 640 nm. (d) NSET-4 (QD-**9**/Au-**15**): [QD-**9**] = 6 nM, [Au-**15**] = 120 nM; total volume 100 μL, PBS pH = 7.4; incubation time = 1 h; RT; [**22**/**23**/**25**] = 0−250 nM; incubation time = 1 min; λ_{exc} = 450 nm; λ_{em} = 640 nm. All experimental values are aggregates of three parallel experiments.

tration useful for efficient NSET process and then studied how selective and sensitive these mixtures were as Sia biosensors.

To screen binding of different sialoglycans, four sialic acid monosaccharides (**16**−**19**) and five sialoglycans (**21**−**25**) were used representing the most common terminal-sialylated structures (Figure 4 and Table 1). Using NSET-1 (**6**/**13**) as a donor/acceptor mixture, a uniform increase in the fluorescence upon the addition of 100 and 150 nM of compounds **16** and **17** and saturation in the signal at 600 and 700 nM was observed (Supporting Information, Figure S2). A similar experiment with compound **18** displayed much more sensitive gain in fluorescence compared to compound **19**, indicating sensitivity of the LFA toward α-sialic acid species. On the basis of these results, the detection limit and detection range for free sialic acid were determined (Table 1).

In contrast, increasing concentration of sialylated glycans **21**, **22**, and **24** resulted in a rapid concentration-dependent increase in fluorescence (Figure 5a). The detection limit for these sugars was in the range of 0.4−0.5 nM (Table 1). Moreover, the LFA binding trend is similar for α2−3- and α2−6-linked sialoglycans. To test for sialic acid sensitivity of human CD22-Fc, the NSET-2 (**7**/**13**) mixture was treated with 1−

dx.doi.org/10.1021/ac400320n | *Anal. Chem.* 2013, 85, 3864−3870

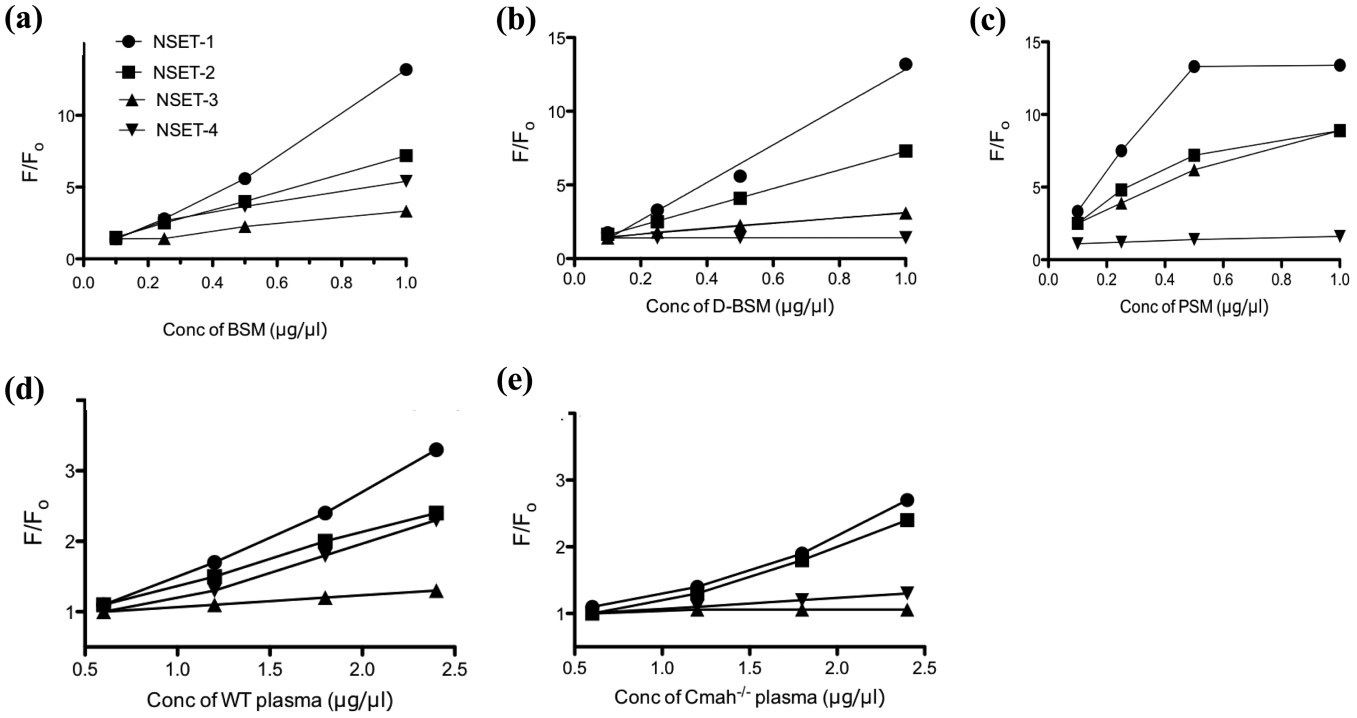

Figure 6. Variation of the fluorescence intensity ratio F/F_0 as a function of the molar biological samples fractions (x). Solvent: PBS; [NSET-1 to 4] remain the same as in Figure 2. (a) [BSM] = 0.1−1 μg/μL; total volume = 100 μL; incubation time = 1 min; λ_{exc} = 450 nm; λ_{em} = 640 nm; (b) [D-BSM] = 0.1−1 μg/μL; total volume = 100 μL; incubation time = 1 min; λ_{exc} = 450 nm; λ_{em} = 640 nm; (c) [PSM] = 0.1−1 μg/μL; total volume = 100 μL; incubation time = 1 min; λ_{exc} = 450 nm; λ_{em} = 640 nm; (d) [WT plasma] = 0.6−2.4 μg/μL; total volume = 100 μL; incubation time = 1 min; λ_{exc} = 450 nm; λ_{em} 640 nm; (e) [$Cmah^{-/-}$ plasma] = 0.6−2.4 μg/μL; total volume = 100 μL; incubation time = 1 min; λ_{exc} = 450 nm; λ_{em} = 640 nm. All experimental values are aggregates of three parallel experiments.

300 nM of **21**, **22**, and **24**, respectively. By plotting the relative fluorescence increase (F/F_0) versus Sia concentration, binding isotherms were obtained (Figure 5b). As expected, **21** did not show any binding. Similar experiments with NSET-3 (**8**/**14**) and NSET-4 (**9**/**15**) mixtures resulted in noticeable preferential fluorescence gain with Neu5Gc and 9-OAc-sialic acid specific glycans, respectively (Figure 5, parts c and d). The detection limits for compounds **22**, **24**, and **25** were calculated based on these results and found to be 0.2 and 1.2 nM, respectively. We observed two phases of fluorescence gain: a uniform rapid fluorescence gain, which can be interpreted as a simultaneous displacement of weakly bound glyco−AuNPs from immobilized SBP and a high affinity of the sugars for protein, and a slow gain that might be due to bulkiness of gold nanoparticles not allowing high-affinity sugars to displace effectively. Finally, the detection limit measured by this method was compared to other QD-based sugar biosensors (Supporting Information, Table S7).[20]

The selectivity of donor/acceptor mixture toward sialoglycans was further demonstrated using a series of solutions (water and PBS solution) containing one or a mixture of representative metals (Na^+, K^+, Ca^{2+}, Zn^{2+}, and Cu^{2+}) or amino acids (leucine, alanine, glycine, aspartic acid, and glutamic acid) or sugars (glucose, maltose, lactose, and dextran) none of which gave fluorescence (Supporting Information, Table S4). The QD/Au mixture can be used to detect the amount of sialic acids with 90−98% accuracy, even after several weeks at −20 °C, showing the stability of the method. The change in accuracy is due to the aggregation of nanoparticles and decrease in the quantum yield of the QDs.

After establishing that the QD-NSET method can quantify synthetic sialoglycan sensitively, we evaluated the applicability of these nanobiosensors to determine the various compositions of sialic acids in biological samples. We used model glycoproteins and different sera with a wide range of sialic acid compositions. An array of four NSET mixtures carrying specific SBP−sialic acid moieties was exposed to PBS solution containing 0.1, 0.25, 0.5, and 1.0 μg/μL solution of bovine submaxillary mucin (BSM), de-O-acetylated (D-BSM) and porcine submaxillary mucin (PSM) solutions, respectively, and change in fluorescence intensity was recorded after 1 min of exposure time. The quantification of sialic acid content in biosamples was derived from the standard curve obtained with the NSET mixture and standard sialoglycan compounds **21**−**25** (Figure 6 and Supporting Information Table S5). Upon addition of BSM to NSET-1 mixture in PBS, a concentration-dependent spontaneous fluorescence gain is observed, indicating that sialic acid moieties on BSM successfully displace AuNPs **13**, and the resultant fluorescence gain indicates the total sialic acid concentration in a given sample. Alternatively, when BSM was added to NSET-2 mixture in PBS, an enhancement of the fluorescence was relatively lower than that of NSET-1 mixture, indicating the amount of α2−6 sialoglycans is around 58−76% of the total sialic acid concentration. A similar experiment with NSET-3 resulted in a smaller fluorescence increase indicating the amount of Neu5Gc is around 21−41% of the total sialic acid. In contrast, NSET-4 showed a large gain in the fluorescence, because 62−71% of the sialic acids in BSM are 9-O-acetylated (Figure 6a). Finally, the Sia concentration measured by this method was

dx.doi.org/10.1021/ac400320n | *Anal. Chem.* 2013, 85, 3864−3870

compared to the data obtained by the standard DMB-HPLC method (Table 2 and Supporting Information Table S6).

Table 2. Comparison of Results with QD-NSET and DMB-HPLC Analysis: Protein Concentration of Mouse Serum = 70 μg/μL Protein[a]

sample	method	total Sia (pmol/μg)	Neu5Gc (% of total sialic acid)	9-OAc-Sia (% of total sialic acid)
bovine submaxillary mucin (BSM)	DMB	300	22	55
	QD-NSET	309 ± 11	21–41	62–71
porcine submaxillary mucin (PSM)	DMB	603	84	10
	QD-NSET	294 ± 7 (0.5 μg)	70–79	7–21
WT mouse blood plasma	DMB	12.2	70	4
	QD-NSET	12 ± 4	50–60	13–31
Cmah$^{-/-}$ mouse blood plasma	DMB	9.7	1	29
	QD-NSET	8 ± 3	1–10	31–53

[a]All experimental values are aggregates of three parallel experiments.

The fluorescence gain in NSET-1, -2, and -4 with D-BSM was almost identical to BSM. However, NSET-3 showed very weak fluorescence since base treatment eliminates most 9-OAc groups, leaving a free OH form (Figure 6b). In contrast, in PSM, the fluorescence was saturated after 0.5 μg/μL sample. This shows that PSM has more sialoglycans compare to BSM and D-BSM samples, and NSET-4 showed significant fluorescence gain indicating a smaller percent of the Sias are 9-O-acetylated (Figure 6c).

After successfully studying the sialic acid compositions in model glycoproteins, we performed the same experiments with blood plasma samples from wild-type and *Cmah*$^{-/-}$ mice. Figure 6, parts d and e, displays NSET mixture behavior at different concentrations of biological samples. As expected, wild-type plasma contains 67–74% α2–6 sialoglycans, 13–31% 9-O-acetylation, and 50–60% Neu5Gc, respectively (Supporting Information, Table S6). Finally, QD-NSET analysis showed that *Cmah*$^{-/-}$ plasma sialic acid contains 66–88% α2–6 sialoglycans, 31–53% 9-O-acetylated, and 1–10% Neu5Gc sugars, respectively (Supporting Information, Table S6). Importantly, all these values are in reasonably close agreement with more precise quantitation obtained with the DMB-HPLC method.

CONCLUSIONS

In conclusion, we have developed a single-step and rapid QD-NSET-based methodology for direct detection of different compositions of sialic acids in biological samples. Our methodology is based on sialic acid specific carbohydrate–protein interactions. The sensitivity of the sensor depends on the SBP that is employed. Using LFA, we detected total concentration of sialic acid in a given sample. CD22, CIgY-Anti-Neu5Gc, and BoCoV were able to detect different linkages and forms of sialic acids. An array containing all these four SBP NSET mixtures would render high-throughput detection of different forms of sialic acid composition in a single platform.

ASSOCIATED CONTENT

Supporting Information

Additional information as noted in text. This material is available free of charge via the Internet at http://pubs.acs.org.

AUTHOR INFORMATION

Corresponding Author

*E-mail: a1varki@ucsd.edu.

Present Addresses

[‖]Department of Chemistry, Indian Institute of Science Education and Research, Pune-411021, India.

[⊥]Department of Cell Research and Immunology, Tel Aviv University, Tel Aviv 69978, Israel.

[▽]National Glycoengineering Research Center, Shandong University, Jinan, Shandong 250012, People's Republic of China.

[○]Department of Medical Microbiology, Nijmegen Centre for Molecular Life Sciences and Nijmegen Institute for Infection, Inflammation and Immunity, Radboud University Nijmegen Medical Centre, Nijmegen, Netherlands.

Notes

The authors declare no competing financial interest.

ACKNOWLEDGMENTS

This work is supported by NIH Grant GM32373 to A.V., GM076360 to X.C., and ECHO Grants of the Council for Chemical Sciences of The Netherlands Organization for Scientific Research (NWO–CW). This work was also supported by an ISEF postdoctoral fellowship to V.P.-K.

REFERENCES

(1) Hakomori, S. *Cancer Res.* **1996**, *56*, 5309.

(2) (a) Angata, T.; Varki, A. *Chem. Rev.* **2002**, *102*, 439–469. (b) Varki, A.; Cummings, R. D.; Esko, J. D.; Freeze, H. H.; Stanley, P.; Bertozzi, C. R.; Hart, G. W.; Etzler. M. E. *Essentials of Glycobiology*, 2nd ed.; Cold Spring Harbor Press: Cold Spring Harbor, NY, 2009; pp 199–218. (c) Chen, X.; Varki, A. *ACS Chem. Biol.* **2010**, *5*, 163.

(3) (a) Schauer, R. *Curr. Opin. Struct. Biol.* **2009**, *19*, 507. (b) Varki, A. *Trends Mol. Med.* **2008**, *14*, 351.

(4) (a) Powell, L. D.; Varki, A. *J. Biol. Chem.* **1994**, *269*, 10628. (b) Brinkman-Van der Linden, E. C. M.; Sjoberg, E. R.; Juneja, L. R.; Crocker, P. R.; Varki, N.; Varki, A. *J. Biol. Chem.* **2000**, *275*, 8633.

(5) (a) de Groot, R. J. *Glycoconjugate J.* **2006**, *23*, 59. (b) Schwegmann-Wessels, C.; Herrler, G. *Glycoconjugate J.* **2006**, *23*, 51.

(6) (a) Kim, Y. J.; Varki, A. *Glycoconjugate J.* **1997**, *14*, 569–576. (b) Cazet, A.; Julien, S.; Bobowski, M.; Krzewinski-Recchi, M. A.; Harduin-Lepers, A.; Groux-Degroote, S.; Delannoy, P. *Carbohydr. Res.* **2010**, *345*, 1377.

(7) (a) Tangvoranuntakul, P.; Gagneux, P.; Diaz, S.; Bardor, M.; Varki, N.; Varki, A.; Muchmore, E. *Proc. Natl. Acad. Sci. U.S.A.* **2003**, *100*, 12045–12050. (b) Hedlund, M.; Padler-Karavani, V.; Varki, N. M.; Varki, A. *Proc. Natl. Acad. Sci. U.S.A.* **2008**, *105*, 18936. (c) Taylor, R. E.; Gregg, C. J.; Padler-Karavani, V.; Ghaderi, D.; Yu, H.; Huang, S.; Sorensen, R. U.; Chen, X.; Inostroza, J.; Nizet, V.; Varki, A. *J. Exp. Med.* **2010**, *207*, 1637–1646. (d) Varki, A. *Glycoconjugate. J.* **2009**, *26*, 231.

(8) Pham, T.; Gregg, C. J.; Karp, F.; Chow, R.; Padlaer-Karavani, V.; Cao, H.; Chen, X.; Witztum, J. L.; Varki, N. M.; Varki, A. *Blood* **2009**, *10*, 5225.

(9) Padler-Karavani, V.; Hurtado-Ziola, N.; Pu, M.; Yu, H.; Huang, S.; Muthana, S.; Chokhawala, H. A.; Cao, H.; Secrest, P.; Friedmann-Morvinski, D.; Singer, O.; Ghaderi, D.; Verma, I. M.; Liu, Y.-T.; Messer, K.; Chen, X.; Varki, A.; Schwab, R. *Cancer Res.* **2011**, *71*, 3352–3363.

(10) (a) Levonis, S. M.; Kiefel, M. J.; Houston, T. A. *Chem. Commun.* **2009**, 2278. (b) James, T. D.; Sandanayake, K. R. A. S.; Shinkai, S. *Nature* **1995**, *374*, 345. (c) Badugu, R.; Lakowicz, J. R.; Geddes, C. D. *Talanta* **2005**, *65*, 762.
(11) Hara, S.; Takemori, Y.; Yamaguchi, M.; Nakamura, M.; Ohkura, Y. *Anal. Biochem.* **1987**, *164*, 138.
(12) (a) Ianniello, R. M.; Yacynyeh, A. M. *Anal. Chem.* **1981**, *53*, 2090. (b) Cao, L.; Ye, J.; Tong, L.; Tang, B. *Chem.—Eur. J.* **2008**, *31*, 9633. (c) Tang, B.; Cao, L.; Xu, K.; Zhuo, L.; Ge, J.; Li, Q.; Yu, L. *Chem.—Eur. J.* **2008**, *14*, 3637−3644. (d) Li, X.; Zhou, Y.; Zheng, Z.; Yue, X.; Dai, Z.; Liu, S.; Tang, Z. *Langmuir* **2009**, *25*, 6580. (e) Aslan, K.; Zhang, J.; Lakowicz, J. R.; Geddes, C. D. *J. Fluoresc.* **2004**, *14*, 391. (f) Aslan, K.; Lakowicz, J. R.; Geddes, C. D. *Anal. Biochem.* **2004**, *330*, 145. (g) Rossi, L. M.; Quach, A. D.; Rosenzweig, Z. *Anal. Bioanal. Chem.* **2004**, *380*, 606. (h) Zhang, Y.; Mali, B. L.; Aitken, C.; Geddes, C. D. *J. Fluoresc.* **2013**, *23*, 187. (i) Dragen, A. I.; Albrecht, M. T.; Pavlovic, R.; Keane-Myers, A. M.; Geddes, C. D. *Anal. Biochem.* **2012**, *425*, 54. (j) Thanh, N. T.; Rosenzweig, Z. *Anal. Chem.* **2002**, *74*, 1624. (k) El-Ansary, A.; Faddah, L. M. *Nanotechnol., Sci. Appl.* **2010**, *3*, 65.
(13) (a) Persson, B.; Long, N. *Phys. Rev. B* **1982**, *26*, 5409. (b) Li, M.; Wang, Q.; Shi, X.; Hornak, L.; Wu, N. *Anal. Chem.* **2011**, *83*, 7061. (c) Li, M.; Cushing, S. K.; Wang, Q.; Shi, Z.; Hornak, L. A.; Hong, Z.; Wu, N. *J. Phys. Chem. Lett.* **2011**, *2*, 2125. (d) Singh, M. P.; Strouse, G. F. *J. Am. Chem. Soc.* **2010**, *132*, 9383. (e) Jennings, T. L.; Schlatterer, J. C.; Singh, M. P.; Greenbaum, N. L.; Strouse, G. F. *Nano Lett.* **2006**, *6*, 1318.
(14) (a) Yu, H.; Chokhawala, H.; Karpel, R.; Yu, H.; Wu, B.; Zhang, J.; Zhang, Y.; Jia, Q.; Chen, X. *J. Am. Chem. Soc.* **2005**, *127*, 17618. (b) Yu, H.; Huang, S.; Chokhawala, H.; Sun, M.; Zhang, H.; Chen, X. *Angew. Chem., Int. Ed.* **2006**, *12*, 3938.
(15) Miller, R. L.; Cannon, J. D., Jr. *Prog. Clin. Biol. Res.* **1984**, *157*, 31.
(16) (a) Chen, W. C.; Completo, G. C.; Sigal, D. S.; Crocker, P. R.; Saven, A.; Paulson, J. C. *Blood* **2010**, *115*, 4778. (b) Razi, N.; Varki, A. *Proc. Natl. Acad. Sci. U.S.A.* **1998**, *95*, 7469.
(17) (a) Zeng, Q.; Langeris, M. A.; vanVliet, A. L.; Huizinga, E. G.; de Groot, R. J. *Proc. Natl. Acad. Sci. U.S.A.* **2008**, *105* (26), 9065. (b) Padler-Karavani, V.; Song, X.; Yu, H.; Hurtado-Ziola, N.; Huang, S.; Muthana, S.; Chokhawala, H. A.; Cheng, J.; Verhagen, A.; Langereis, M. A.; Kleene, R.; Schachner, M.; de Groot, R. J.; Lasanajak, Y.; Matsuda, H.; Schwab, R.; Chen, X.; Smith, D. F.; Cummings, R. D.; Varki, A. *J. Biol. Chem.* **2012**, *287*, 22593−22608.
(18) Diaz, S. L.; Padler-Karavani, V.; Ghaderi, D.; Hurtado-Ziola, N.; Yu, H.; Brinkman-Van der Linden, E. C. M.; Varki, A.; Varki, N. *PLoS ONE* **2009**, *4*, 4241. (b) Padler-Karavani, V.; Hurtado-Ziola, N.; Pu, M.; Yu, H.; Huang, S.; Muthana, S.; Chokhawala, H. A.; Cao, H.; Secrest, P.; Friedmann-Morvinski, D.; Singer, O.; Ghaderi, D.; Verma, I. M.; Liu, Y. T.; Messer, K.; Chen, X.; Varki, A.; Schwab, R. *J. Biol. Chem.* **2011**, *71*, 3352.
(19) (a) Kikker, R.; Lepenies, B.; Adibekian, A.; Laurino, P.; Seeberger, P. H. *J. Am. Chem. Soc.* **2009**, *18*, 2110. (b) Patel, P. C.; Giljohann, D. A.; Daniel, W. L.; Zheng, D.; Prigodich, A. E.; Mirkin, C. A. *Bioconjugate Chem.* **2010**, *21*, 2250. (c) Thaxton, C. S.; Hill, H. D.; Georganopoulou, D. G.; Stoeva, S. I.; Mirkin, C. A. *Anal. Chem.* **2005**, *77*, 8174. (d) Orbach, M.; Lahav, M.; Milko, P.; Wolf, S. G.; Van der Boom, M. E. *Angew. Chem., Int. Ed.* **2012**, *51*, 7142. (e) Wang, H.; Chen, L. O.; Shen, X.; Zhu, L.; He, J.; Chen, H. *Angew. Chem., Int. Ed.* **2012**, *51*, 8021.
(20) (a) Tang, B.; Cao, L.; Xu, K.; Zhuo, L.; Ge, J.; Li, Q.; Yu, L. *Chem.—Eur. J.* **2008**, *14*, 3637. (b) Dai, Z.; Kawde, A.-N.; Xiang, Y.; La Belle, J. T.; Gerlach, J.; Bhavanandan, V. P.; Joshi, L.; Wang, J. *J. Am. Chem. Soc.* **2006**, *128*, 10018.

Supporting Information

for

Quantum Dot-Nanometal Surface Energy Transfer Based Biosensing of Sialic Acid Compositions and Linkages in biological Samples

Raghavendra Kikkeri,[†,Δ] Vered Padler-Karavani,[†] Sandra Diaz,[†] Andrea Verhagen,[†] Hai Yu,[⊥] Hongzhi Cao,[⊥,▽] Martijn A. Langereis, [£,±] Raoul J.De Groot, [£] Xi Chen,[⊥] Ajit Varki[†*]

*

[†]Glycobiology Research and Training Center, Departments of Medicine and Cellular & Molecular Medicine, University of California, San Diego, La Jolla, California, USA.

[£]Virology Division, Department of Infectious Diseases & Immunology, Faculty of Veterinary Medicine, Utrecht University, Yalelaan 1, 3584 CL Utrecht, The Netherlands.

[⊥]Department of Chemistry, University of California, Davis, California 95616, USA

Present addresses

[Δ]Department of Chemistry, Indian Institute of Science Education and Research, Pune-411021, India.

[±]Department of Medical Microbiology, Nijmegen Centre for Molecular Life Sciences and Nijmegen Institute for Infection, Inflammation and Immunity, Radboud University Nijmegen Medical Centre, Nijmegen, Netherlands.

[□]National Glyco-engineering Research Center, Shandong University, Jinan, Shandong 250012, P. R. China

[†] Current address: [Δ]Department of Chemistry, Indian Institute of Science Education and Research, Pune-411021. [±]Department of Medical Microbiology, Nijmegen Centre for Molecular Life Sciences and Nijmegen Institute for Infection, Inflammation and Immunity, Radboud University Nijmegen Medical Centre, Nijmegen, Netherlands. [□]National Glycoengineering Research Center, Shandong University, Jinan, Shandong 250012, P. R. China, [#]Department of Cell Research and Immunology, Tel Aviv University, Tel Aviv 69978, Israel

[*]Correspondence should be address to A.V. (a1varki@ucsd.edu).

General Information

All chemicals used were reagent grade and used as supplied except where noted. Analytical thin layer chromatography (TLC) was performed on Merck silica gel 60 F254 plates (0.25 mm). Compounds were visualized by UV irradiation or dipping the plate in $KMnO_4$ solution followed by heating. Column chromatography was carried out using force flow of the indicated

solvent on Fluka Kieselgel 60 (230–400 mesh). ^{1}H and ^{13}C NMR spectra were recorded on a Varian VXR-400 (300 MHz) spectrometer. Mass spectra were performed by the Mass Spectrometry-service at the Glycotechnology CORE Resource, UCSD, San Diego. DL-thioctic acid was purchased from Fluka. PEG reagents were purchased from Nektar Therapeutics, Huntsville, USA. Absorption spectra were recorded using a microplate spectrophotometer fitted with Hellma filters (Hellma, 041.002-UV) and an immersion probe made of quartz suprazil (Hellma, 661.500-QX). Fluorescence emissions were recorded on a Molecular Devices spectrofluorometer. *N*-Glycolylneuraminic acid (Neu5Gc) was synthesized from mannosamine hydrochloride, introducing the glycolyl moiety to yield *N*-glycolylmannosamine (ManNGc), which was enzymatically converted to Neu5Gc as described previously[1]. The α2-3- and α2-6-linked sialylglycans and 9-OAc sialylglycan pairs (**12**, **21–25)** were synthesized using an efficient one-pot three-enzyme chemoenzymatic synthetic system[2] containing an *E. coli* K-12 sialic acid aldolase, an *N. meningitidis* CMP-sialic acid synthetase[1], and a sialyltransferase selected from a *Pasteurella multocida* multifunctional sialyltransferase[3] or a *Photobacterium damsela* α2–6-sialyltransferase[4]. These sialosides were then conjugated to biotinylated human serum albumin (HSA) at pH 7.5 using a homobifunctional adipic acid *p*-nitrophenyl ester[5] as an efficient linker, then purified and confirmed by matrix assisted laser desorption ionization – time of flight (MALDI-TOF). *N*-Glycolylneuraminic acid α/βOMe (**18–19)** were synthesized as described previously[6,7]. *Limax flavus* agglutinin (LFA), a sialic acid binding protein was purchased from Calbiochem, CD22 and Chicken-IgY anti-Neu5Gc (CIgY-Anti-Neu5Gc) were prepared as described previously[8,9]. Recombinant soluble bovine coronavirus hemagglutinin-esterase with the esterase function mutated was prepared as described[10]. Porcine or Bovine submaxillary mucins (PSM or BSM, respectively) were prepared as described previously[11]. The BCA protein assay reagent was a product of Pierce (Rockford, IL). The sialic acid content and the purity of all glycoconjugates on gold nanoparticles were further confirmed by 1,2-diamino-4,5-methylenedioxybenzene–high performance liquid chromatography (DMB–HPLC) as described herein.

Synthesis of Quantum dots (6–9).

Synthesis of QDs

CdSe/ZnS quantum dots with an emission maximum centered at 610 nm were synthesized *via* pyrolysis of the oragonometallic procedure [12].

Synthesis of QD-COOH (1).

DL-thioctic acid (0.5 g, 2.45 mmol) was dissolved in ethanol/water (1:1) mixture. Sodium borohydride (0.18 g, 4.8 mmol) was added and stirred at 0 °C for 3 h. The solution was neutralized with 1 N HCl solution, extracted with chloroform, dried over sodium sulfate, concentrated and dissolved in 100 μL of ethanol. Then, 0.1 mL of QDs in chloroform (O.D >50 at 400 nm) was added. The mixture was stirred at 60°C for 12 h. In between, another 50 μL of ethanol was added. QD-COOH were separated by basifying the solution with potassium tert-butoxide. Centrifugation at 3000 rpm for 3 mins yielded a dark pellet. This pellet was separated and dissolved in distilled water (1 mL), centrifuged at 3000 rpm for 3 mins to yield a clear solution.

Concentration of QDs was estimated using a previously published procedure[13].

Synthesis of QD (6–9).

Quantum dots (**1**) (50 μM in PBS, pH 7.3), *N*-hydroxysuccinimide (NHS; 20 mg, 0.17 mmol) and EDC (6 mg, 0.03 mmol) were added to distilled water, and stirred at room temperature for 3 h. The active ester was added to sialic acid binding proteins (1 μg/μL, 20–50 μL). The mixture was incubated at 25 °C for 2 h under shaking in the dark and then kept overnight at 4 °C. No obvious precipitation occurred after this conjugation reaction. Both the free nonconjugated QDs and the byproduct isourea were removed by ultra-filtration using 30 KD Microcon centrifugal devices by centrifugation at 3000 rpm for 5 min. The filter retentate, containing QD-SBP, was dissolved in 0.1 mL PBS buffer, and additionally purified using 100 KD Microcon centrifugal device by centrifugation at 3000 rpm for 5 min. The conjugate was recovered with 0.1 mL of PBS and transferred to a new Eppendorf tube and then stored at 4 °C in the dark until use. Concentration of QDs was estimated using a previously published procedure[13]. The protein concentration was measured using the BCA Protein Assay Kit from Pierce [14].

Synthesis of Compounds (10) & (11).

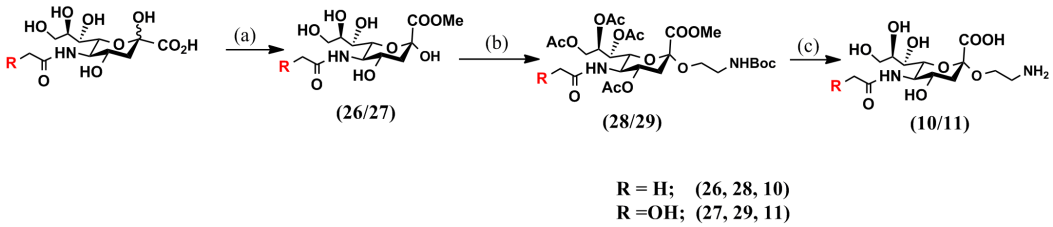

Figure S1. Reagents and conditions (a) Amberlite-H^+/MeOH; (b) AcCl/AcOH; *N*-Boc ethanol-amine /AgOTf ; (c) TFA/$CHCl_3$, NaOH/MeOH.

(a) **Methyl 5-acetamido-3,5-dideoxy D-glycoro-D-galacto-2-nonulopyranosonate (26).**

N-Acetylneuraminate (1 g, 3.23 mmol) and Amberlite-H^+ (2 g) were dissolved in methanol (10 mL) and stirred at room temperature for 12 h. The solvent was filtered and the resin was washed with methanol, the organic layer was concentrated *in vacuo* and afforded the desired product (**26)** (0.89 g, 84% yield) and product was used as such for the next step.

Methyl 5-glycolylamido-3,5-dideoxy D-glycero-D-galacto-2-nonulopyranosonate (27).

Compound (**27)** was obtained in 81% (0.16 g) starting from Neu5Gc (0.2 g, 0.61 mmol) using the similar method as described above for compound (**26)** and product was used as such for the next step (Figure S1).

(b) 5-Acetamido 4,7,8,9-tetra-*O*-acetyl 3,5-dideoxy-2-ethanol-*N*-Boc amido-D-glycoro-D-galacto-2-nonulosonic acid methyl ester (28). Compound (**26)** (0.5 g, 1.5 mmol) was dissolved in 4 mL acetic acid/acetyl chloride (1:4) and stirred at 0°C

for 3 h under nitrogen atmosphere. Then, it was stirred for 48 h at room temperature under N_2 atmosphere. The solvent was evaporated under reduced pressure and the resulting oil was dissolved in anhydrous acetonitrile (20 mL). To this mixture *N*-Boc ethanol amide (0.75 g, 4.5 mmol) and silver triflate (0.6 g, 2.2 mmol) were added and stirred at room temperature for 48 h. The organic layer was washed with saturated sodium thiosulfate and saturated brine, and dried by anhydrous sodium sulfate. The resultant crude mixture was evaporated *in vacuo* and purified by flash silica column chromatography to yield compound (**28)** (α:β = 3 :1) (75 mg, 21%) R_f = 0.5 ($CHCl_3$/MeOH 96:4),

^{1}H NMR (400 MHz, $CDCl_3$): δ 5.37 (m, 2H), 5.31 (d, *J* = 7.6 Hz, 1H), 5.28 – 5.14 (m, 1H), 4.87 (dq, *J* = 14.0, 4.8 Hz, 1H), 4.29 (dd, *J* = 12.4, 2.4 Hz, 1H), 4.10 (m, 4H), 3.81 (s, 3H), 3.67 – 3.55 (m, 1H), 3.51 (q, *J* = 5.6, 4.8 Hz, 1H), 3.48 – 3.39 (m, 2H), 2.63 (dd, *J* = 12.8, 4.6 Hz, 1H), 2.14 (s, 6H), 2.04 (s, 3H), 2.03 (s, 3H), 1.88 (s, 3H). 1.21 (s, 9H) ^{13}C NMR (100 MHz, $CDCl_3$): δ 171.2, 170.3, 170.1, 168.0, 167.4, 95.4, 73.1, 68.8, 68.2, 67.9, 65.6, 62.2, 61.7, 53.0, 51.5, 49.2, 30.7, 30.3, 25.9, 20.8, 20.6; HRMS: m/z: calc'd for $C_{27}H_{42}N_2NaO_{15}$ (M+ Na) 657.2483, found 657.2481.

5-Glycolylamido 4,7,8,9-tetra-*O*-acetyl 3,5-dideoxy-2-ethanol-*N*-Boc amido-D-glycero-D-galacto-2-nonulosonic acid methyl ester (29). Compound (**29)** was obtained in 15% (27 mg) (α:β = 3 :1) starting from compound **27** (0.15 g, 0.44 mmol) using the similar method as described above (Figure S1) for compound **28** R_f = 0.5 ($CHCl_3$/MeOH 96:4), ^{1}H NMR (400 MHz, $CDCl_3$): δ 5.90 (d, *J* = 9.6 Hz, 1H), 5.41 – 5.29 (m, 2H), 5.24 (qt, *J* = 7.6, 4.4 Hz, 1H), 4.92 (td, *J* = 12.0, 4.4 Hz, 1H), 4.57 (d, *J* = 15.2 Hz, 2H), 4.32 – 4.22 (m, 2H), 4.18 – 4.00 (m, 3H), 3.80 (s, 3H), 3.58 (dt, *J* = 11.6, 6.2 Hz, 1H), 3.49 (dt, *J* = 9.6, 5.6 Hz, 1H), 3.43 (q, *J* = 8.0, 7.2 Hz, 2H), 2.62 (dd, *J* = 12.8, 4.4 Hz, 1H), 2.13 (s, 3H), 2.12 (s, 3H), 2.02 (s, 3H), 2.01 (s, 3H), 1.89 (s, 3H), 1.23(s, 9H). ^{13}C NMR (100 MHz, $CDCl_3$): δ 171.1, 170.9, 170.8, 170.7, 169.6, 97.4, 74.9, 74.3, 70.6, 70.3, 69.5, 67.1, 64.1, 61.1, 52.2, 49.1, 37.9, 31.6, 27.2, 22.7, 21.6, 21.2; HRMS: m/z: calc'd for $C_{29}H_{44}N_2NaO_{17}$ (M+ Na) 715.2538, found 715.2536.

(c) (2-Ethanolamine)-3,5-dideoxyl-D-glycero-β-D-galacto-2-nonulosonic acid 10. 50 mg of compound (**28)** was dissolved in dry chloroform (5 mL) and 1 mL of trifluoroacetic acid. After 1h, solvent was evaporated and dissolved in dry methanol (5 mL) and NaOMe (1 M in methanol, 50 μL) was added. After 6 h, the Amberlite-acid resin (1.0 g) was added and stirred for 10 min. The reaction mixture was filtered and the filtrate was concentrated to give the desired product (**10)** as a yellow oil (23 mg, 82% yield). ^{1}H NMR (400 MHz, CD_3OD) 4.71-4.66 (m, 1H), 3.94-3.74 (m, 6H), 3.72 (t, *J* = 8.0 Hz, 1H), 3.56 (d, *J* = 10.0 Hz, 1H), 3.41 (t, *J* = 10.0 Hz, 1H), 3.22-3.20 (m, 1H), 2.60 (d, *J*=4.8 Hz, 1H), 1.90 (s, 3H). ^{13}C-NMR (100 MHz, D_2O) δ 174.90, 91.22, 82.5, 76.4, 71.6, 70.6, 69.2, 68.1, 66.7, 63.7, 60.8, 48.5, 38.1, 35.8, 20.8. HRMS: m/z: calc'd for $C_{13}H_{24}N_2NaO_9$ (M+ Na^+) 375.1380, found 375.1384.

(2-Ethanolamine)-3,5-dideoxyl-D-glycero-β-D-galacto-2-nonulosonic acid (11). Compound (**11)** was obtained in 65% (12

mg) starting from compound (**29)** (30 mg) using the similar method as described above (Figure S1) for compound **10**. ^{1}H NMR (400 MHz, CD_3OD): 4.72-4.66 (m, 1H), 4.11 (d, 2H), 3.85- 3.77 (m, 2H), 3.71-3.66 (m, 5H), 3.65-3.56 (m, 2H), 3.51 (t, *J* = 10 Hz, 2H), 2.62 (d, *J*=4.8Hz, 1H); ^{13}C-NMR (100 MHz, D_2O): 175.6, 97.8, 96.5, 90.3, 84.9, 75.6, 73.2, 71.3, 70.1, 69.7, 67.3, 64.2, 49.3, 43.2, 35.7. ; HRMS: m/z: calc'd for $C_{13}H_{24}N_2NaO_{10}$ ($M+Na^+$) 391.1329, found 391.1331.

Synthesis of AuNPs (13-15).

Synthesis of gold nanoparticles with S-PEG$_{2000}$-COOH

A solution of PEGylated thio (100 mg, 0.05 mmol) in MeOH (1 mL) was added to a solution of tetrachloroauric acid (5 mg, 0.01 equiv) in water. $NaBH_4$ (19 mg, 0.5 mmol) in water was then added in small portions with rapid shaking. The black suspension formed was shaken for an additional 2 h and the solvent was then removed. The residue was dissolved in 5 mL of nanopure water and was purified by Millipore centrifugal filtering (Centriplus Mol Wt. 30 KD, 1 h, 3000 x g). The process was repeated until the nanoparticles were free of salts and starting material. The residue in the Centriplus filter was dissolved in water (2 mL). Concentration of AuNP was estimated using a previously published procedure. ^{1}H NMR (300 MHz, D_2O): 3.72–3.52 (br. 164H), 3.12 (t, *J* = 7.6 Hz, 2H), 2.89–2.84 (m, 2H). ^{13}C-NMR (75 MHz, D_2O): 78.2, 73.6, 73.1, 71.3, 70.3, 31.1, 20.7.

Synthesis of AuNPs (13-15).

To a solution of PEGylated AuNP (60 μM) in water (2 mL), EDC (12 mg, 0.06 mmol) and NHS (18 mg, 0.18 mmol) were added. After 2 h, compound **6/7/8** was added and stirred at room temperature for 12 h. Finally 2-ethanol amine (20 μL) was added to quench the unreacted carboxylic acid. Both the free sialic acid and byproduct isourea were removed by ultra-filtration using 30 KD Microcon centrifugal devices by centrifugation at 3000 rpm for 5 min. The filter retentate, containing AuNP, was dissolved in 1 mL nanopure water, and additionally purified using 100 KD Microcon centrifugal device by centrifugation at 3000 rpm for 5 min. The conjugate was recovered with 1 mL of PBS and transferred to a new Eppendorf tube and then stored at 4 °C in the dark until used. Concentration of AuNP was estimated using a previously published procedure. The sialic acid concentration was measured using the DMB-HPLC method.

Photophysical Properties of QD (6–9).

The emission spectra of the QDs (**6–9)** are shown in Figure S8 . Upon excitation at 450 nm, a maximum emission at 610–613 nm were observed. Quantum yields have been calculated using the equation,

$$\mathbf{F_{comp}/F_{ref} = A_{comp} * [C]_{ref} / A_{ref} * [C]_{comp}}$$

Where **[C]** refers to the concentration of the samples and **A** to the area of the emission spectra. Here, fluorescein was used as a reference compound of quantum yield $\mathbf{F_{ref}}$ = 0.98. All compounds exhibit a more intense emission.

Table S1. Photophysical data for QDs. [a] I_o = Excitation at max 450 nm; sample was prepared in water.

Compound	λ_{max}	K_{Sv}
6	610	8.7×10^9
7	613	9.4×10^9
8	612	9.4×10^9
9	613	7.2×10^9

Table S2. Quenching constant as measured by exciting QDs at λ_{max} = 450 nm and reading emission at λ_{max} = 610 nm.

	QD-6	**QD-7**	**QD-8**	**QD-9**
Au-13	8.7×10^9 M^{-1}	9.4×10^9 M^{-1}	---	---
Au-14	8.6×10^9 M^{-1}	9.1×10^9 M^{-1}	9.4×10^9 M^{-1}	---
Au-15	N.M	N.M	N.M	7.2×10^9 M^{-1}

Table S3. Concentration of AuNPs affect the NSET signals with respect to QD concentration 6 nM.

NSET	Detection range (nM)	Detection Limit (10^{-7} M)
1 (**6/13**)	30-120	30
2 (**7/13**)	30-120	30
3 (**8/14**)	20-120	20
4 (**9/15**)	20-100	20

DMB-HPLC Assay. The sialic acid (Sia) contents of all the gold nanoparticles and glycoconjugates used were analyzed for their type (acetylated and non-acetylated Neu5Ac or Neu5Gc), quantity and purity. Sias were released from nanoparticles and glycoconjugates by acid hydrolysis using 2 M acetic acid for 3 h at 80 °C. Free Sias were then derivatized with 1,2-diamino-4,5-methylenedioxybenzene (DMB) and analyzed by fluorescence detection by reverse-phase HPLC (DMB-HPLC). Quantification of Sias was done by comparison with known quantities of DMB-derivatized Neu5Ac[15].

Assembly of quantum dots and gold nanoparticles conjugates. Gold nanoparticles **(13–15)** solutions (1–150 nM) was added to quantum dots (**6–9**) solution (6 nM) in a 96-well microtiter plate. After incubating 1 h at RT, fluorescence intensity was recorded, exciting at 450 nm and emission at 610 nm respectively (Table S2).

Quantification of different forms of sialic acids by NSET (1-4): AuNPs (**13–15)** solution (130 to 150 nM) was added to the prepared QDs **6–9** aqueous solution (6 nM) for an equilibration period (1 h) to react completely. Under this condition, the

nanobiosensor NSET-mixture was formed and could be used for the subsequent sialic acid sensing. Afterwards, the above sensing solution was aliquoted into 96-well plates and different concentration of sialic acid scaffolds (**16–25)** were added. After allowing to react for 1 min at RT, 96-well plates was placed in fluorescece plate reader and the fluorescence intensity at 610 nm was recorded by the maximal excitation wavelength at 450 nm. All experiment values represent mean of three independent parallel experiments.

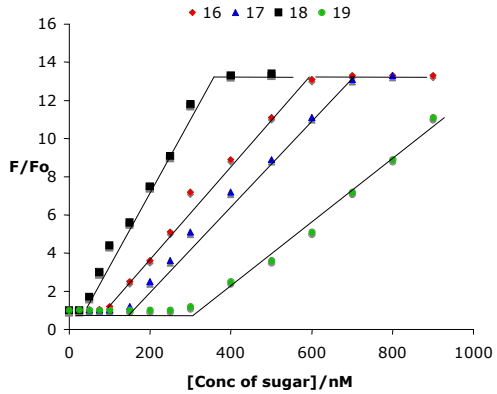

Figure S2. Sialic acid biosensor using different donor/acceptor compositions. Fluorescence increase of **NSET-1** in presence of increasing concentrations of sialic acid residues (**16–19**) [QD-**6**] = 6 nM, [Au-**13**] = 110 nM, total volume 100 µL, PBS pH= 7.4; incubation time = 1 h; RT; [**16-19**] = 0–1000 nM incubation time = 1 min; λ_{exc}= 450 nm; λ_{em}= 610 nm.

Table S4. Summary of analytes and matrices 5 µM, and the corresponding fluorescence changes(F/F_o) at 640 nm of **NSET-1** mixture in PBS solution.

Metals	Amino acids	Sugars
Na^+ (1.02), K^+ (1.02), Ca^{2+} (1.04), Zn^{2+} (1.01), Cu^{2+} (1.02)	Leucine (1.04), alanine (1.01), glycine (1.01) aspartic acid (1.06), glutamic acid (1.06)	Glucose (1.01), maltose (1.01), lactose (1.01), dextrane (1.01).

Table S5. Analytical parameters related to determination of different compositions of sialic acids in biological samples .

Biological samples	Conc (µg/µL)	Total Sialic acid (µM)	α2-6 sialoglycans (pmol/µg)	9-OAc sialoglycans (pmol/µg)	Non-human sialic acid (pmol/µg)
Bovine	0.1	21 ± 4	16 ± 4	15 ± 4	8 ± 3
Submaxillary	0.25	43 ± 9	29 ± 3	31 ± 6	15 ± 4
Mucin (BSM)	0.5	104 ± 7	59 ± 4	65 ± 6	35 ± 4
	1.0	309 ± 11	180 ± 4	193 ± 5	65 ± 4
De-O-acetylated	0.1	21 ± 4	16 ± 4	12 ± 2	14 ± 4
BSM	0.25	57 ± 3	31 ± 4	12 ± 1	29 ± 3
	0.5	97 ± 7	52 ± 4	12 ± 1	38 ± 4
	1.0	275 ± 9	194 ± 12	12 ± 4	63 ± 4
Porcine	0.1	54± 5	38 ± 4	12 ± 2	38 ± 4
Submaxillary	0.25	152 ± 7	79 ± 4	16 ± 2	108 ± 4
Mucin (PSM)	0.5	294 ± 7	153 ± 4	29 ± 5	233 ± 4
	1.0	305 ± 11	232 ± 4	33 ± 4	290 ± 4

WT Mouse Plasma	0.6	6 ± 1	3 ± 1	2 ± 1	3 ± 1
	1.2	21 ± 2	10 ± 1	3 ± 1	8 ± 2
	1.8	27 ± 2	21 ± 2	5 ± 1	20 ± 3
	2.4	51 ± 4	34 ± 3	7 ± 1	31 ± 3
$Cmah^{-/-}$ Mouse Plasma	0.6	6 ± 1	4 ± 1	4 ± 2	3 ± 1
	1.2	18 ± 2	10 ± 2	10 ± 2	4 ± 1
	1.8	25 ± 2	18 ± 2	15 ± 2	4 ± 1
	2.4	43 ± 3	36 ± 2	17 ± 2	4 ± 1

Table S6. Percent composition of different sialic acid in biological samples.

Biological samples	Conc (μg/μL)	Total Sialic acid (μM)	α2-6-sialylglycans (%)	9-OAc sialylglycans (%)	Non-human sialic acid (Neu5Gc) (%)
BSM	0.1–1.0	21–306	58–76	62–71	21–41
De-*O*-acetylated BSM	0.1–1.0	21–298	55–76	4–15	21–45
PSM	0.1–0.5	54-300	51–70	7–21	70–79
WT mouse Plasma	0.6–2.4	6–51	67–74	13–31	50–60
$Cmah^{-/-}$ mouse plasma	0.6–2.4	6–43	66–88	31–53	1–10

Sialic acid detection in glycoproteins and serum: A standard solution of NSET mixtures 1–4 was prepared as described above and freshly prepared glycoproteins and serum solutions were added at different concentration in a 96-well plates. After allowing to react for 1 min at RT, 96-well plates was placed in fluorescece plate reader and the fluorescence intensity at 610 nm was recorded by the maximal excitation wavelength at 450 nm. All experiment values represent mean of three independent parallel experiments.

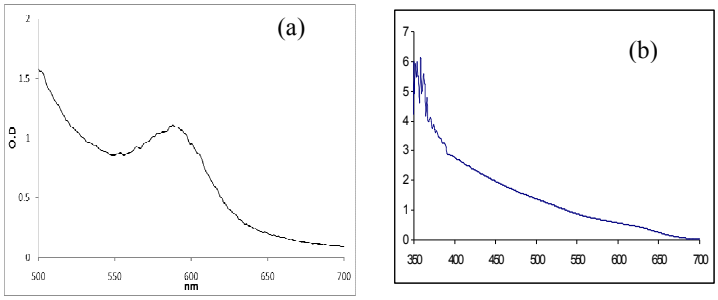

Figure S3. UV-visible (a) QD-LFA (QD-**6**) and (b) AuNP-**13**

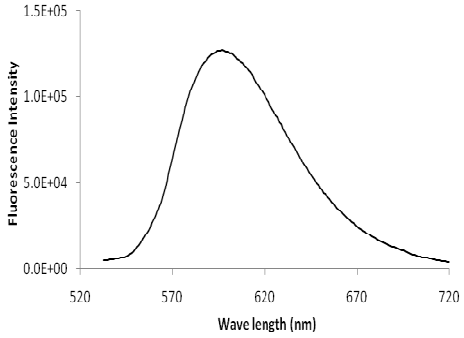

Figure S4. Fluorescence spectra of QD-LFA (QD-**6**).

Transmission Electron Microscopy (TEM).

A drop of the 10 nM concentration sample was deposited on a 400 mesh copper grids coated with nitrocellulose followed by carbon evaporation. The grids were observed in a Philips CM 120 at an accelerating voltage of 200 kV. Figure S11 shows typical TEM images of monodispersed AuNPs **(13)**, QD-CD22-Fc **(7)** and **NSET-2 (13&7)**. A mean diameter 1.5 – 2.3 nm was found for the AuNPs, whereas, mean diameter of QD cappted thioctic acid was around 6-7 nm respectively.

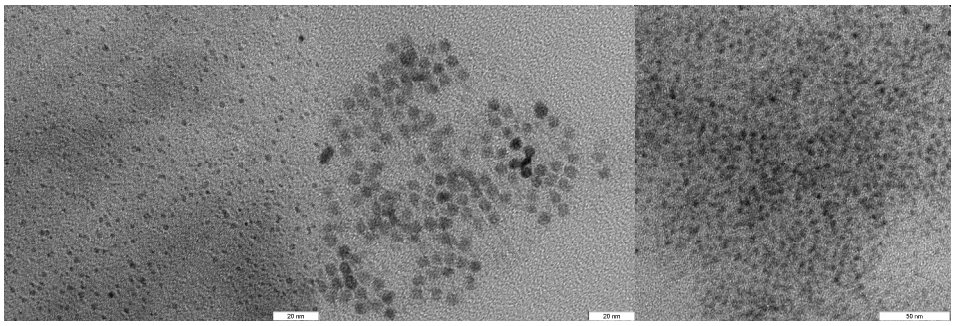

(a) **(b)** **(c)**

Figure S7: TEM images of nanoparticles : (a) TEM of gold nanoparticles (**13**) (scale range 20 nm); (b) TEM of quantum dots nanoparticles (**7**) (scale range 20 nm); (c) TEM of NSET-2 with AuNPs (**13**) and QD (**7**) (scale range 50 nm).

Table S7: Detection limits of sugars by nanoparticles based methods.

Methods	Detection limits (M)	Ref
AuNPs-enzyme conjugates	10^{-4}	16
PtNPs-H2O2 oxidation	10^{-2}	17
Quantum dots/lectin interactions	10^{-6}	18

References.

1. Yu, H., Yu, H., Karpel, R., Chen, X. *Bioorg. Med. Chem.* **2004**, 12, 6427–6435.
2. Yu, H., Chokhawala, H. A., Huang, S., Chen, X. *Nat. Protoc*. **2006**, 1, 2485-2492.
3. Yu, H., Chokhawala, H., Karpel, R., Yu, H., Wu, B., Zhang, J., Zhang, Y., Jia, Q., Chen, X., *J. Am. Chem.Soc*. **2005**, 127, 17618-17619.
4. Yu, H., Huang, S., Chokhawala, H., Sun, M., Zhang, H., Chen, X., *Angew. Chem. Int. Ed. Engl.* **2006**, 12, 3938.
5. Yu, H., Chokhawala, H. A., Varki, A., Chen, X. *Org. Biomol. Chem.* **2007**, **5**, 2458-2463.
6. Pham, T., Gregg, C. J., Karp, F., Chow, R., Padler-Karavani, V., Cao, H., Chen, X., Witztum, J. L., Varki, N. M., Varki, A. *Blood*, **2009**, 114, 5225–5235.
7. Padler-Karavani, V., Hurtado-Ziola, N., Pu, M., Yu, H., Huang, S., Muthana, S., Chokhawala, H.A., Cao, H., Secrest, P., Friedmann-Morvinski, D., Singer, O., Ghaderi, D., Verma, I.M., Liu, Y.-T., Messer, K., Chen, X., Varki, A., Schwab, R., *Cancer Res.*, **2011**, 71, 3352-3363.
8. Zhang, M., Varki, A. *Glycobiology.* **2004**, **14**, 939-949.
9. Diaz, S.L., Padler-Karavani, V., Ghaderi, D., Hurtado-Ziola, N., Yu, H., Brinkman-Van der Linden, E.C.M., Varki, A and Varki, N.M. *PLoS ONE.* **2009**, 4, 4241.
10. Zeng, Q., Langeris, M. A., vanVliet, A. L., Huizinga, E. G., de Groot, R. J. *Proc. Natl. Acad. Sci. U. S. A.,* **2008***,* 105, 26, 9065–9069.
11. Tangvoranuntakul, P., Gagneux, P., Diaz, S., Bardor, M., Varki, N.M., Varki, A., and Muchmore, E.: *Proc Natl Acad Sci U S A.* **2003**, **100**, 12045-12050.
12. Xie, R., Kolb, U., Li, J., Basche, T., Mews, A., *J. Am. Chem. Soc*., **2005**, 127, 7480-7488.
13. Leutherdale, C. A., Woo, W. K., Mikulec, F. V., Bawendi, M. G., *J. Phys. Chem. B* **2002**, 106, 7619–7622.
14. Radford, M. M, *Anal. Bio. Chem.* **1976**, 72, 248–254.
15. Hara, S., Yamaguchi, M., Takemori, Y., Nakamura, M.,Ohkura, Y., *J Chromatogr*. **1986**. 377, 111–119.
16. Bahshi, L., Frasconi, M., Telvered, R., Yehezkeli, O., Willner, I. *Anal. Chem*. **2008**, 80, 8253
17. Sato, K., Kodama, D., Anzai, J. -I., *Anal. Bioanal. Chem.* **2006**, 386, 1899.
18. (a) Dai, Z., Kawde, A.-N., Xiang, Y., La Belle, J. T., Gerlach, J., Bhavanandan, V. P., Joshi. L., Wang, J., *J. Am. Chem. Soc* **2006,** 128, 10018l; (b) Tang, B., Cao, L., Xu, K., Zhuo, L., Ge. J., Li, Q., yu, L., *Chem. Eur. J*. **2008**, 14, 3637; (c) Dai, Z., Kawde, A-N., Xiang, Y., La Belle, J. T., Gerlach, J., Bhavanandan, V. P., Joshi, L., Wang. J. *J. Am. Chem. Soc*. **2006**, 128, 10018.

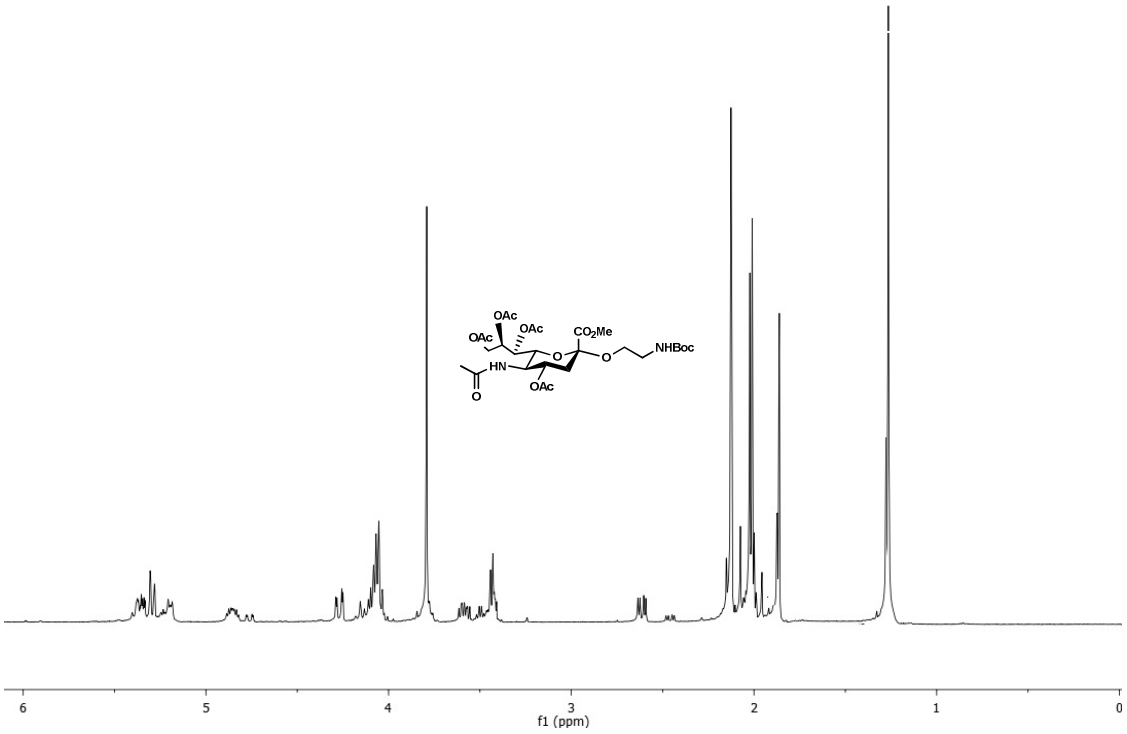
OAc
OAc
OAc
CO2Me
NHBoc
HN
O
OAc
O
6
5
4
3
2
1
0
f1 (ppm)

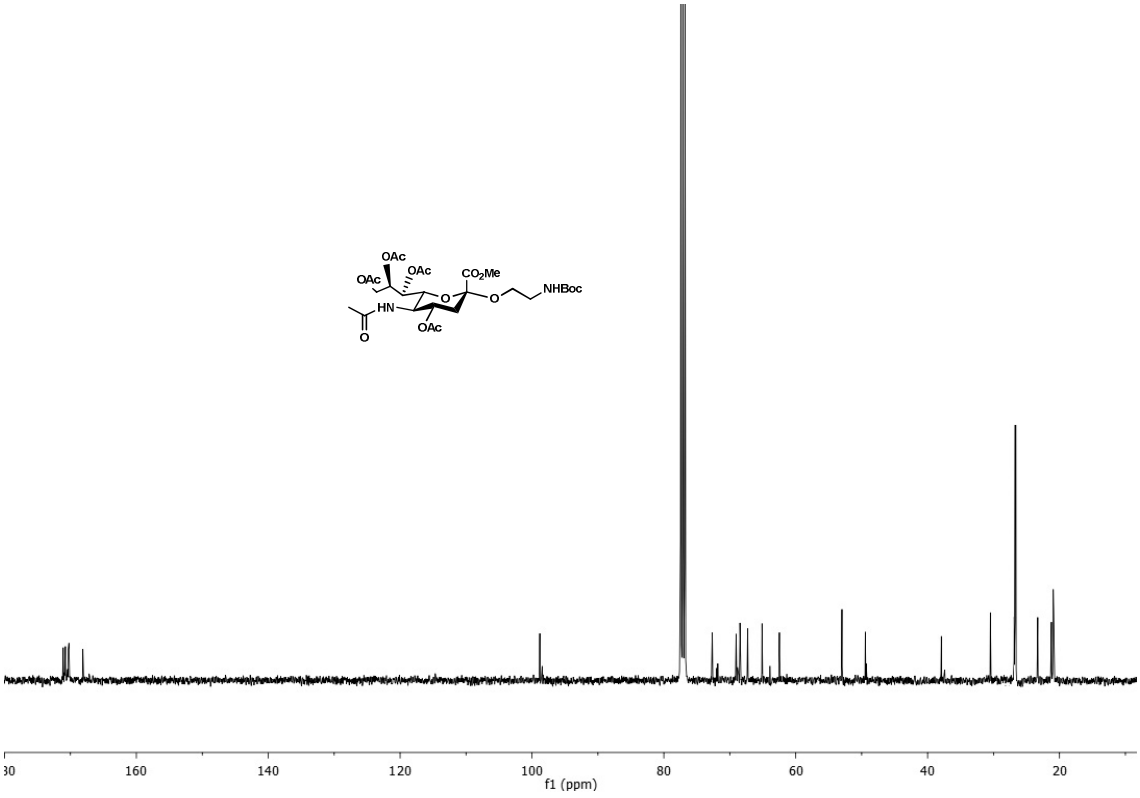
OAc
OAc
OAc
CO2Me
NHBoc
HN
O
OAc
O
160
140
120
100
80
60
40
20
f1 (ppm)

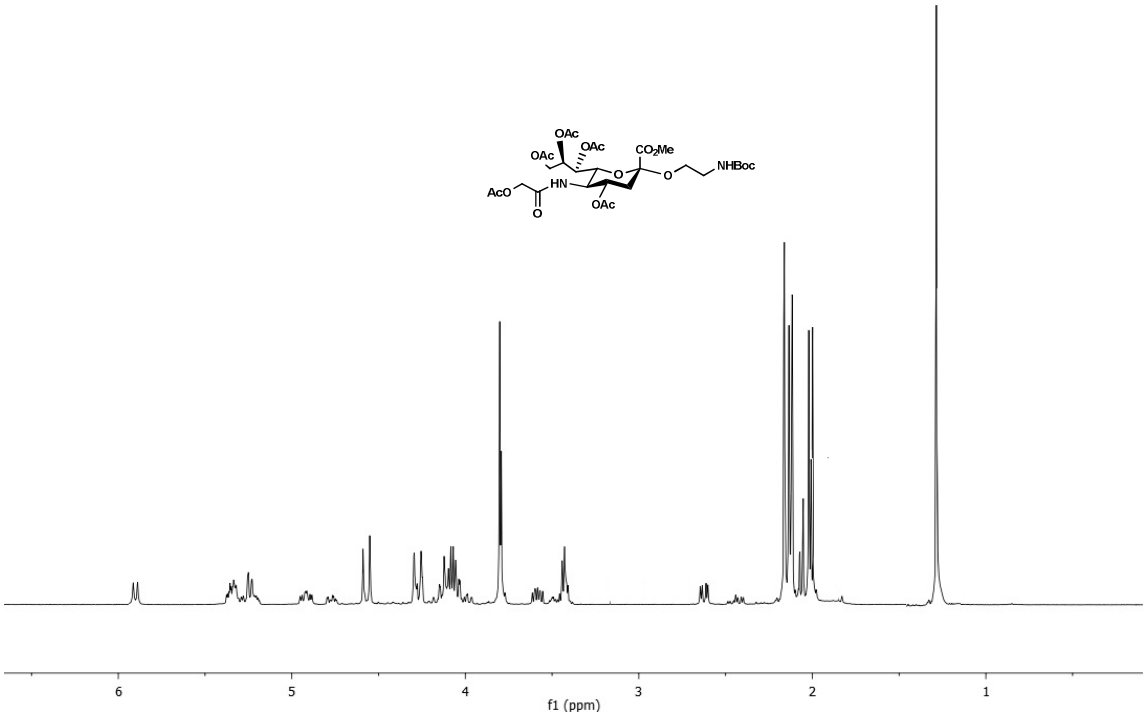
OAc
OAc
OAc
CO2Me
NHBoc
AcO
HN
O
O
OAc
6
5
4
3
2
1
f1 (ppm)

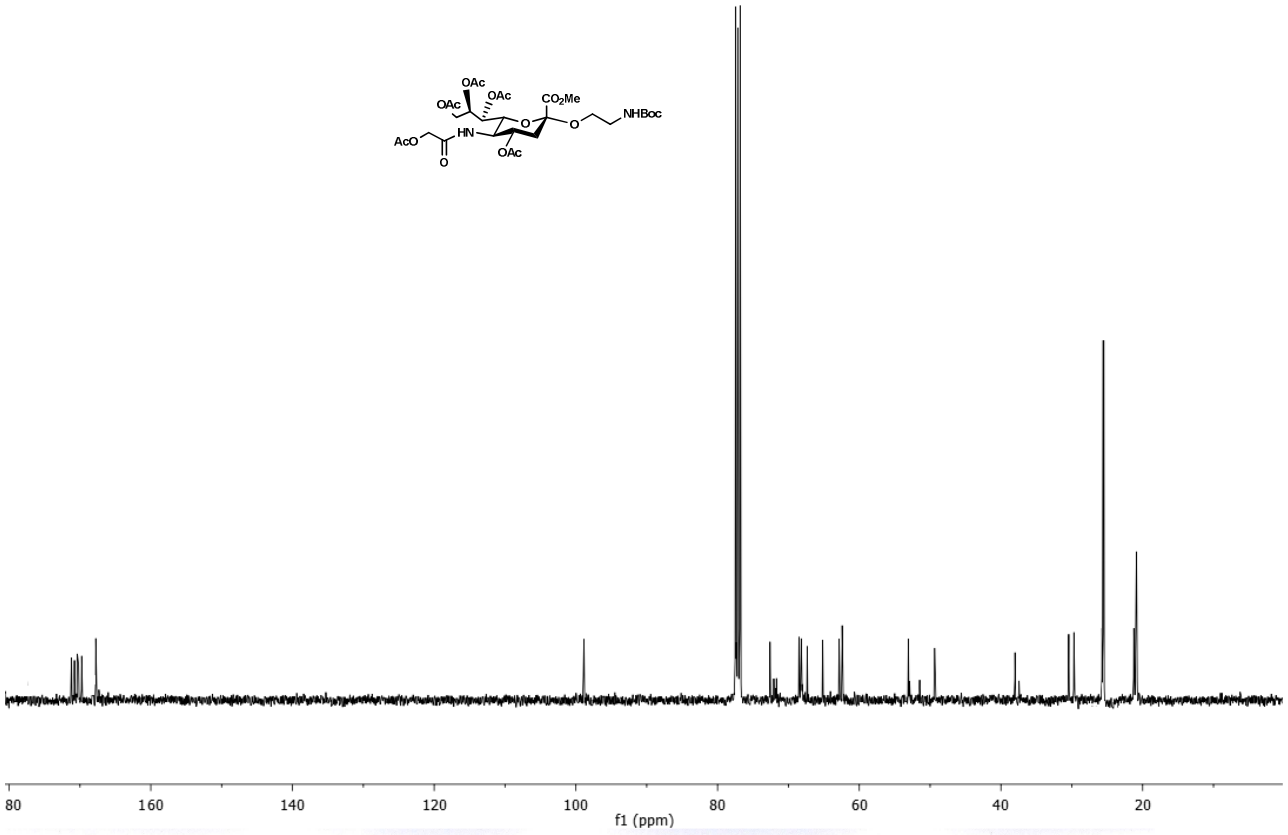
OAc
OAc
OAc
CO2Me
NHBoc
AcO
HN
O
OAc
O
80
160
140
120
100
80
60
40
20
f1 (ppm)

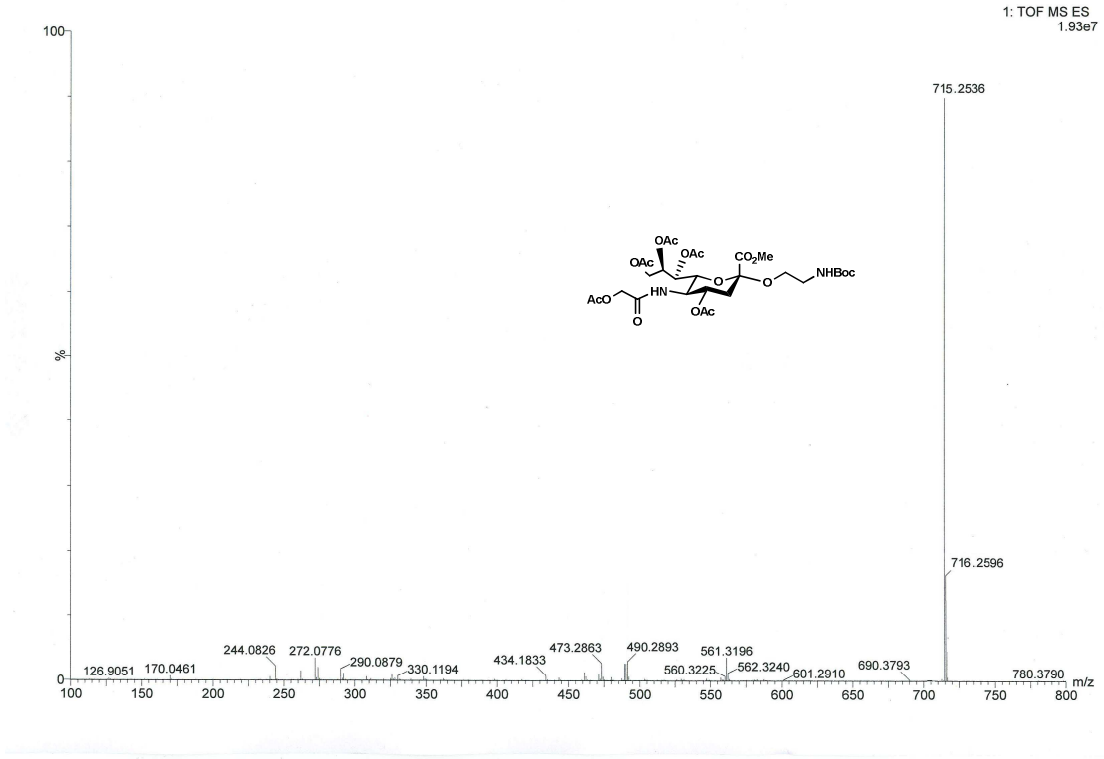
1: TOF MS ES
1.93e7
100
%
0
715.2536
716.2596
244.0826
272.0776
290.0879
330.1194
434.1833
473.2863
490.2893
561.3196
560.3225
562.3240
601.2910
690.3793
780.3790
126.9051
170.0461
100
150
200
250
300
350
400
450
500
550
600
650
700
750
800
m/z

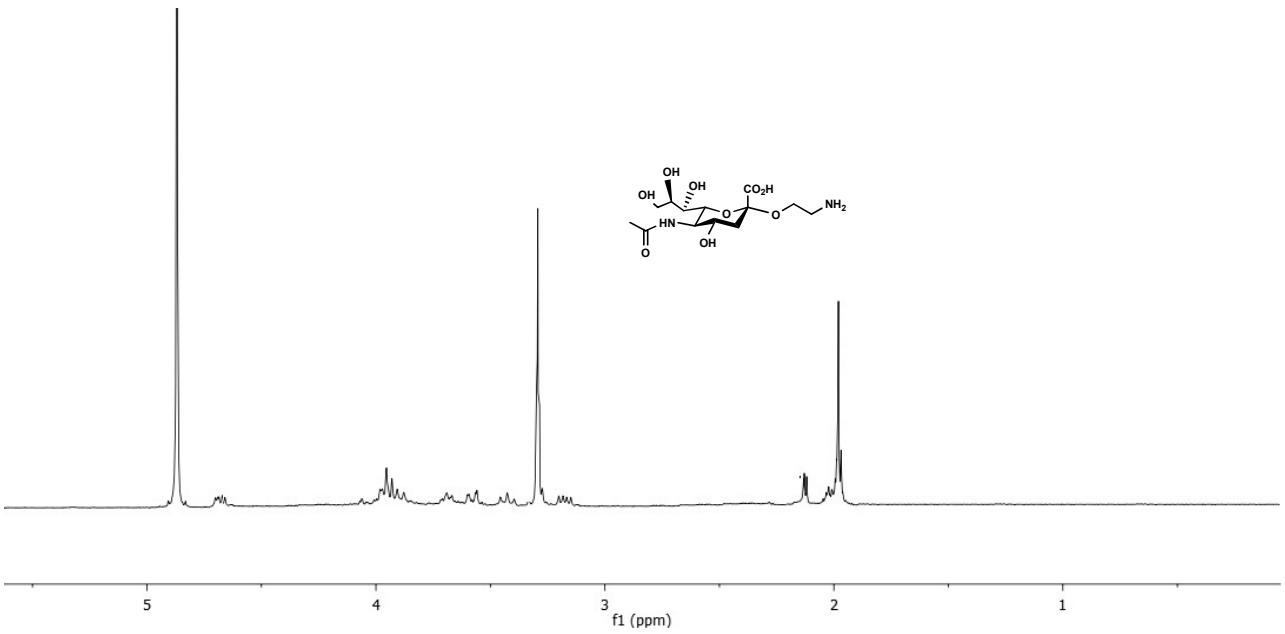
OH
OH
OH
CO2H
NH2
HN
O
OH
O
5
4
3
2
1
f1 (ppm)

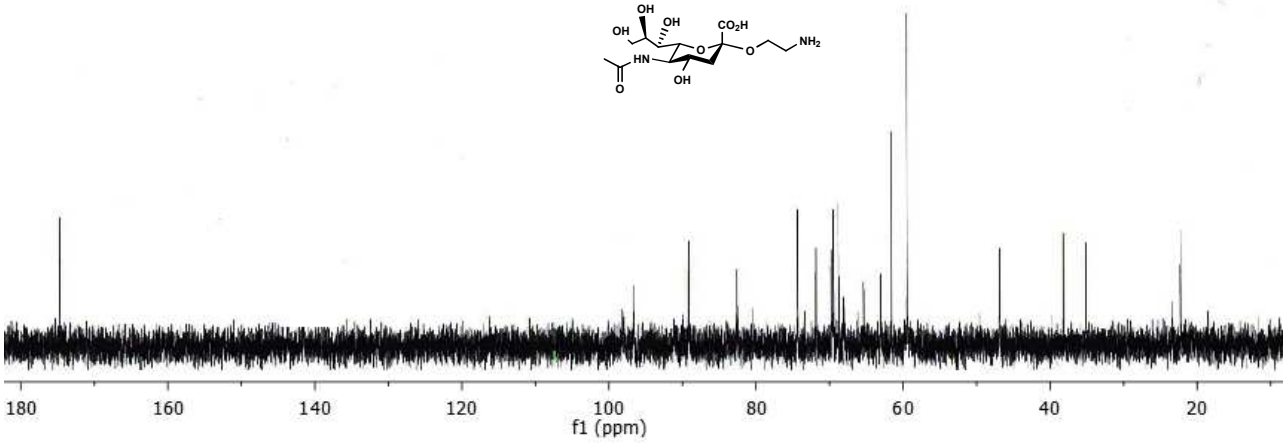
OH
OH
OH
CO2H
NH2
HN
O
OH
O
180
160
140
120
100
80
60
40
20
f1 (ppm)

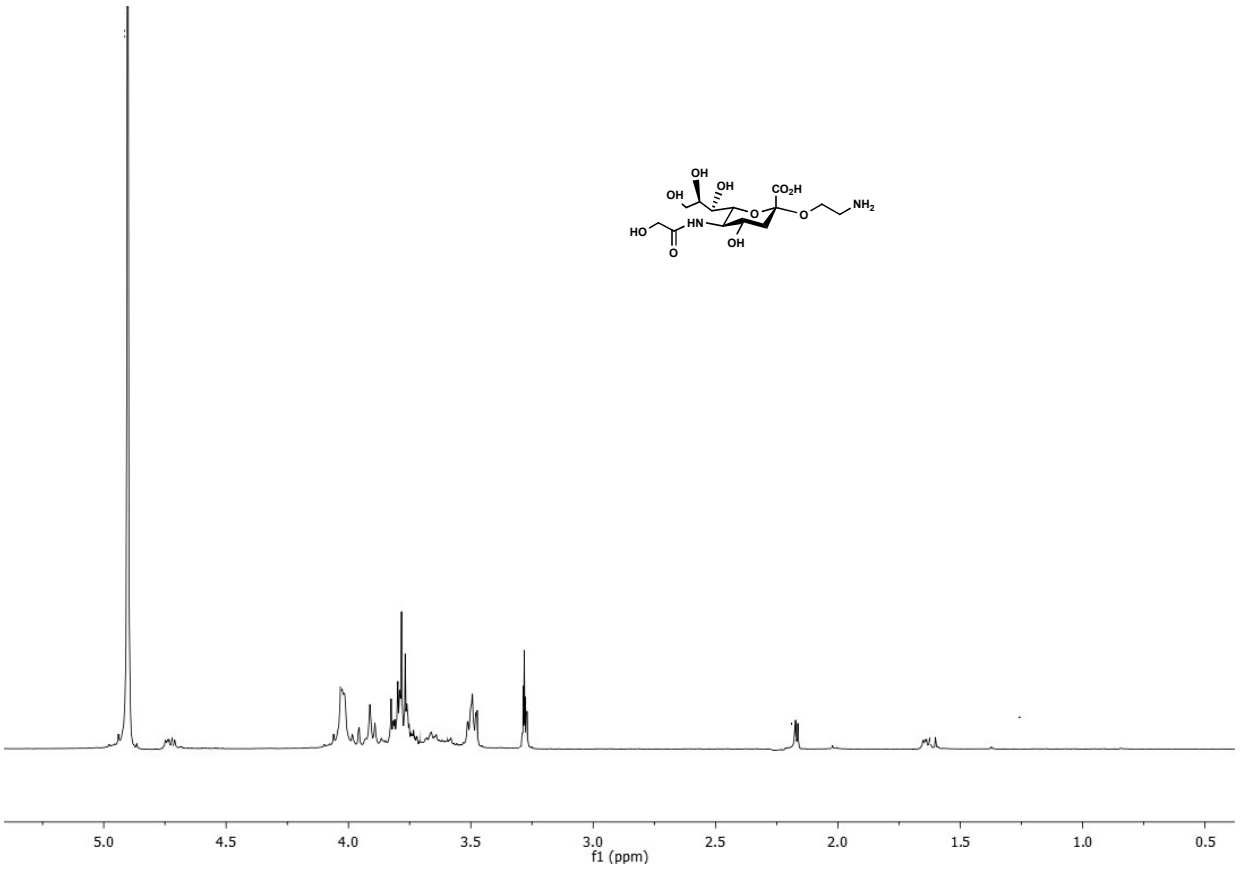
OH
OH
OH
CO2H
NH2
O
HO
HN
O
OH
5.0
4.5
4.0
3.5
3.0
2.5
2.0
1.5
1.0
0.5
f1 (ppm)

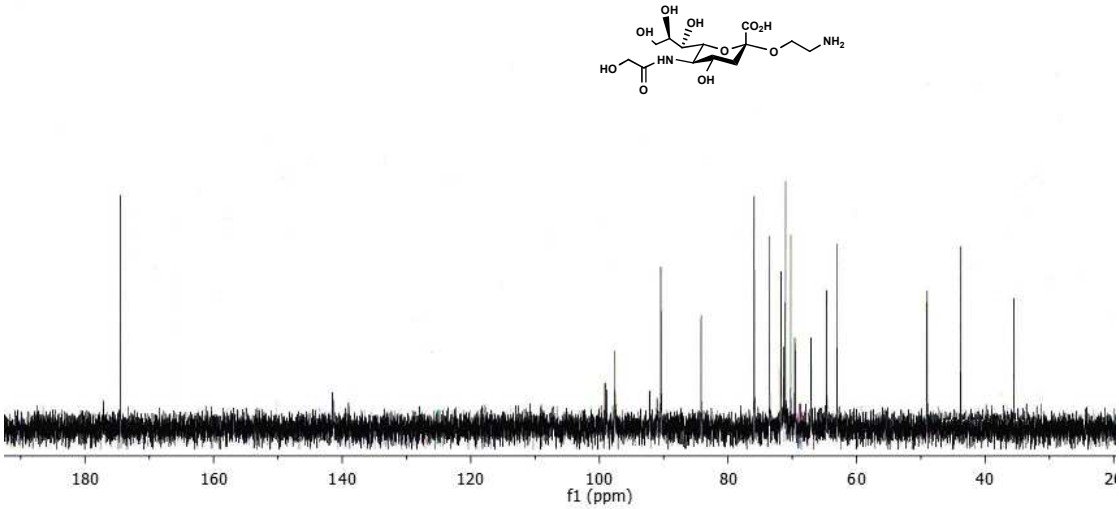
OH
OH
OH
CO2H
NH2
O
HO
HN
O
OH
180
160
140
120
100
80
60
40
f1 (ppm)

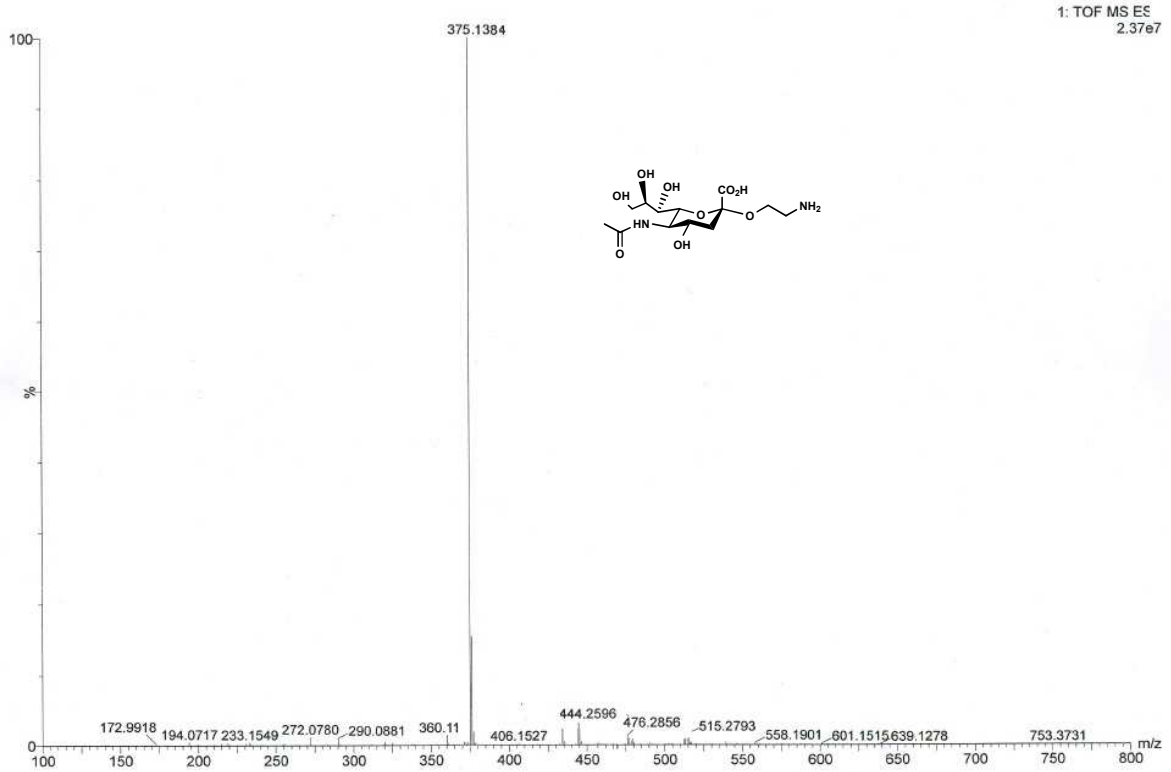
1: TOF MS ES
2.37e7
100
%
0
375.1384
172.9918
194.0717
233.1549
272.0780
290.0881
360.11
406.1527
444.2596
476.2856
515.2793
558.1901
601.1515
639.1278
753.3731
m/z
100
150
200
250
300
350
400
450
500
550
600
650
700
750
800
OH
OH
OH
CO2H
NH2
HN
O
O
O
OH
O

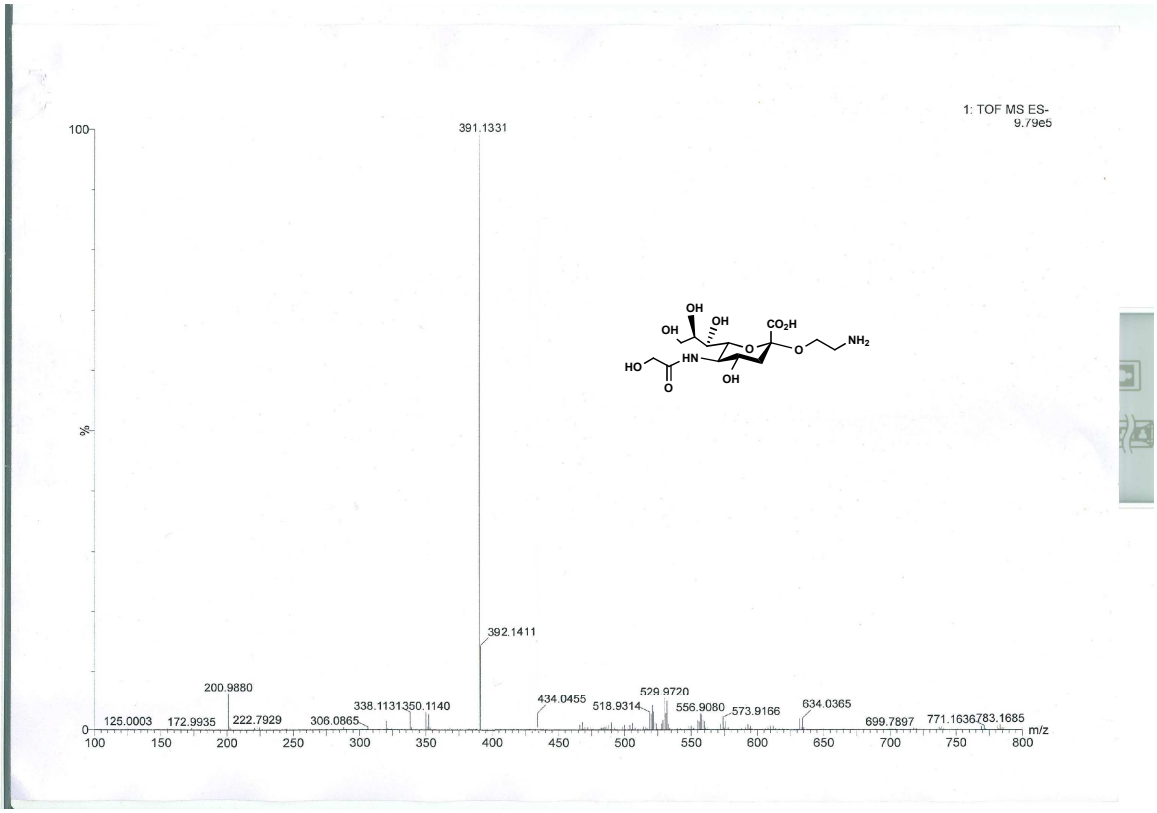
1: TOF MS ES-
9.79e5
100
%
0
391.1331
392.1411
200.9880
125.0003
172.9935
222.7929
306.0865
338.1131
350.1140
434.0455
518.9314
529.9720
556.9080
573.9166
634.0365
699.7897
771.1636
783.1685
m/z
100
150
200
250
300
350
400
450
500
550
600
650
700
750
800
OH
OH
OH
CO2H
NH2
HO
HN
O
O
O
OH

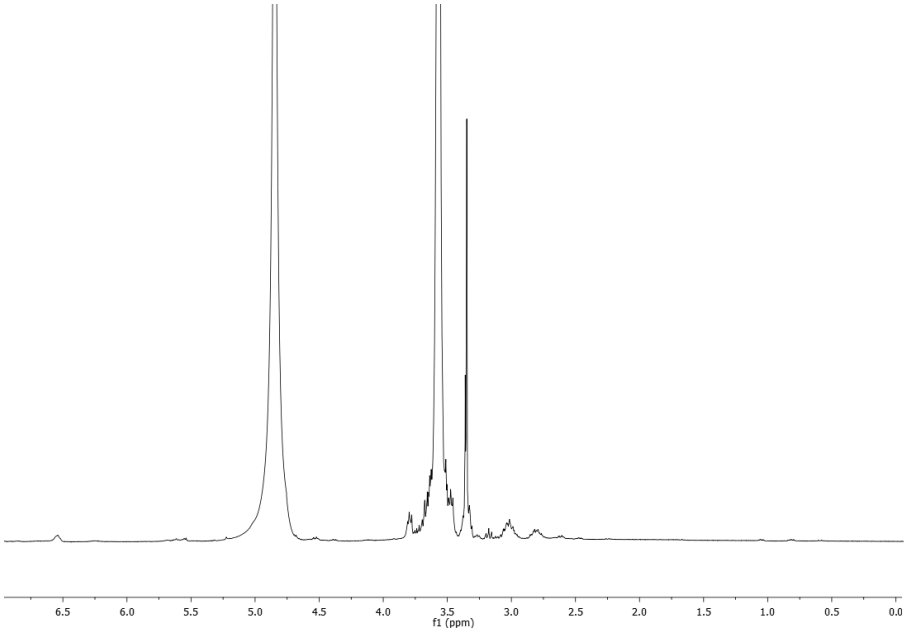

Figure S5. ^{1}H-NMR of SH-PEG-COOH coated gold nanoparticles